Separation and Purification Technology 278 (2022) 119295

Contents lists available at ScienceDirect

Separation and Purification Technology

journal homepage: www.elsevier.com/locate/seppur

# Zeolite membranes: Synthesis and applications

Catia Algieri *, Enrico Drioli

*Institute on Membrane Technology, National Research Council of Italy (ITM–CNR), Cubo 17C, Via Pietro Bucci, 87036 Rende, CS, Italy*

ARTICLE INFO

*Keywords:*
Zeolite membranes
Synthesis
Pervaporation
Desalination
Gas separation
Zeolite membrane reactors

ABSTRACT

Membrane-based technology has attracted considerable attention owing to its low energy consumption, mild operating conditions, and high efficiency. Polymeric membranes are widely utilized in different separation processes for their low cost and highly reproducible preparation. Fouling and the trade-off between permeability and selectivity represent the main drawbacks in the polymeric membrane field. These problems could be overcome by using inorganic membranes that are less prone to fouling due to their hydrophilic nature, high chemical stability, and high permeability and selectivity. Zeolite membranes, a type of inorganic membranes, can separate liquid and gas species (with very similar size and shape) thanks to their defined pore size at a molecular level and high adsorption property. They are studied in different separation processes as gas separation, pervaporation, and desalination. However, they find application, at the industrial level, only for alcohol dehydration by pervaporation process. Indeed, although 30 years are passed since the first scientific papers about the zeolite membrane preparation, many problems are still unsolved, as reproducibility of the synthesis, defects into the zeolite layer, and high manufacturing costs, which caused a limitation to their application on a large scale.

In this review, the main zeolite membrane preparation methods and the novelty in their developing and fabricating have been analyzed. Their application in pervaporation and desalination has been discussed. The effect of zeolite membrane topology and chemical composition on natural gas purification has been presented in detail. The application of zeolite membrane reactors in different interesting processes has been discussed. Concluding remarks and future perspective have been also suggested.

## 1. Introduction

Today, membrane technology represents one of the most interesting routes for developing chemical processes by satisfying the Process Intensification Strategy (PIS) [1]. The main characteristics of the membrane operations that make them in line with the PIS are high efficiency, low energy use, low capital costs, high safety and operational flexibility, and easy scale-up [1,2]. Polymeric membranes are employed in numerous applications as gas separation processes, water purification, desalination, and dialysis [2]. The main drawbacks in this membrane field are the fouling and the trade-off between permeability and selectivity [3]. Inorganic membranes, for their high thermal and mechanical stabilities and interesting separation properties, can be used when polymeric membranes cannot operate [4]. Many efforts have been dedicated to preparing and applying these membranes in different processes as gas separations, pervaporation, reverse osmosis, and catalytic membrane reactors [4]. Zeolite membranes exhibit well-defined pore dimensions at a molecular level, and high adsorption property and so can separate, in a continuous way, liquid and gas species based on molecular sieving effect and adsorption selectivity [5].

Zeolites are crystalline inorganic materials with channels and cavities. The chemical elements present in the zeolite structure are silicon (Si), aluminum (Al), and oxygen (O) disposed of in a tetrahedron (Four oxygen atoms surround Si or Al atoms). The negative charge of Al (being tetracoordinate) is balanced by counter-ions which are alkaline or alkaline earth metals, such as $Na^{+}$, $K^{+,}$ or $Ca^{2+}$ in most cases [6]. These materials show high adsorption property, molecular sieving ability, and ion exchange capacity. For these reasons, zeolites are used at the industrial level for *i.* separation of linear from non-linear hydrocarbons [7], *ii.* removal of heavy metals [8,9], *iii.* reduction of the ammonium excess [10] for water softening [11] and *iv.* gas adsorption [12]. Over the past decades, supported zeolite layers have been prepared and used in gas and liquid separations, catalysis, and sensors [13].

In the last decades, different problems have been solved to improve synthesis reproducibility and understand the relation between membrane microstructure and separation performance. However, many

* Corresponding author.
*E-mail address:* c.algieri@itm.cnr.it (C. Algieri).

https://doi.org/10.1016/j.seppur.2021.119295
Received 18 March 2021; Received in revised form 9 July 2021; Accepted 10 July 2021
Available online 15 July 2021
1383-5866/© 2021 Elsevier B.V. All rights reserved.

issues are still unsolved, such as intercrystalline defects and high production costs, influenced by almost 70% of the support cost [14]. For this reason, today, they are applied at the industrial level only for the dehydration of different organic solvents, and few companies commercialize them, as Jiangsu Nine Heaven Co. Ltd. (China), Inocermic GmbH zeolite membranes. (Germany) and Mitsui Engineering and Shipbuilding (Japan) [15].

In this review, the principal and also recent zeolite membrane preparation methods have been discussed. The use of new calcination procedures and defects curing treatments for improving their performance in various gas and liquid separation processes has been presented. Their application in pervaporation and water desalination processes has been discussed. The attention has also been focused on their use in natural gas purification and as membrane reactors. New important topics as their application in solid-state batteries and Space engineering have been also reviewed. Finally, the challenges in preparing zeolite membranes for a large commercial application have been identified, and future perspectives have also been discussed.

## 2. Zeolite membrane preparation

Zeolites are crystalline aluminosilicates with pore size at a molecular level, good adsorption property, and high thermal and chemical stability. These materials as membranes permit separate gas and liquid mixtures based on molecular sieving effect and the adsorption selectivity [16]. Usually, these membranes are prepared on porous supports for conferring mechanical strength because self-standing layer is very brittle. Supports of different materials (alumina, stainless steel, titania, silica, mullite, and glass) and configurations (flat, mono-channel, multichannel, and hollow fiber) are used [17-19]. At present, there are several methods developed for preparing supported zeolite membranes, and the main are the in situ (called too one-step) and the secondary-growth. In the one-step, the support is immersed in an autoclave in contact with a synthesis solution or gel, and the layer is formed by hydrothermal treatment [20]. This process is activated thermally, and it is affected by the chemical composition and the molar ratio of the different components present in the solution or gel, the pH, and the temperature [21]. This method is not reproducible since nucleation and crystal growth happen simultaneously. The membranes exhibit very low permeance for forming the layer on the surface and in the support pores. The secondary growth method is the most used, and it ensures better control of the zeolite structure formation due to the decoupling the nucleation from the crystal growth [22]. This method includes various steps, the synthesis of the zeolite nuclei, the seeds deposition on the support surface, and growth and the layer stabilization (chemical bound formation between support and crystals) by hydrothermal treatment. Different procedures are used for depositing the zeolite nuclei on the support as: dip-coating [23,24], rubbing [25,26], covalent chemical deposition [27-32] and filtration [33-35]. In the dip-coating, the electrostatic interaction between support and zeolite nuclei is favored by determining the pH where the zeta potential of the two different materials exhibits different signs [36,37]. A cationic polymer can be also adsorbed on the support to have a positive surface charged and so to improve the electrostatic interaction with the zeolite nuclei [38]. During the dip-coating, the seeds fall during the support removal from the zeolite slurry for the gravitational force action [39,40]. Therefore, it is difficult to obtain a uniform layer, and so it is repeated several times with consequent reduction of the reproducibility [41]. More controllable seeding procedure is the varying-temperature hot-dip coating (VTHDC) which includes three steps: (1) hot-dip coating of seeds using a high concentrated seed suspension at high temperature; (2) the removal of big seeds by rubbing off; (3) hot-dip coating using a low concentrated suspension at low temperature [42]. In this case, the seeding is favored by the coupled actions of capillary force and the temperature-driven pressure difference (caused by the air shrink close to the support for the rapid decrease in temperature). The temperature-driven pressure difference drives the large seeds into pinholes or cracks because the action of the capillary force is weak [43]. With the rubbing procedure, the seeds are deposited on the surface of the support by using small brushes, and the layer is not uniform [42]. In 2005, Pera-Titus *et al.* used the cross-flow filtration process for seeding tubular support [33]. The support has been kept fix in the horizontal position, and the layer was not uniform for the negative action of the gravitational force. Algieri *et al.* have obtained a uniform layer by coupling the cross-flow filtration with the rotation of the tubular support (along its longitudinal axis) [39]. The rotation of the support (at low speed for avoiding the action of the shearing forces) permits the deposition of the seeds on the overall surface area of the support. Several research groups studied the possibility of attaching micrometer-sized zeolite crystals on substrates by covalent linkers for obtaining zeolite monolayers [27-31]. This route furnishes well-aligned zeolite monolayers applied in the industry as catalysts, molecular sieves, and chemical sensors [31].

After the seeding, the hydrothermal treatment permits the growth of the seeds and the defects coverage for maximizing the permeance and the separation factor. Traditionally, an appropriate gel is prepared by mixing a silica source, an aluminum source, water, and a template (when it is required). Subsequently, the aging of the gel for a certain period is performed. The seeded alumina support is then immersed in a Teflon-lined autoclave in contact with the gel and heated at a specific temperature value and in a certain period [32,39]. Finally, the film is repeatedlywashed with distilled water up to neutral pH (removing amorphous materials).

A gel-free method avoids different steps as gel preparation, gel aging, washing of the membrane and the Teflon-liner, and the disposal of unreacted gel [43,44]. In 2007, Okubo and coworkers proposed a gel-free one-step method where Si wafers function as support and Si source for the silicalite layer formation [45]. Initially, the wafer was coated with a solution of tetrapropylammonium hydroxide (TPAOH) that acts as a template and base. The wafer-TPAOH system was then treated with steam in an autoclave. As a result, silicalite films with preferential a and b out-of-plane orientations are obtained. A gel-free secondary growth procedure for preparing oriented silicalite films was proposed by Yoon et al. [44]. The authors used a homemade silica disk covered with a monolayer of b-oriented silicalite seeds by rubbing. The coated silica disk has been wetted with a dilute TPAOH solution and then put in an autoclave at 190 °C and at different synthesis times. Membranes characterized by different thicknesses (from 100 nm to 200 nm) are used to separate o- and p-xylene mixtures at two different temperatures (150 and 200 °C). The results are interesting in terms of permeance ad separation factors, indicating that they are almost defect-free. This method is inexpensive and fast, but it is applied on flat supports, while for industrial application, tubular supports are necessary for optimizing the area/volume ratio. Recently, silicalite membranes have been synthesized on seeded tubular silica supports using gel-free steam-assisted conversion method [46]. Briefly, the tubular silica support is seeded with silicalite seeds by electrophoretic deposition. Then, the seeded silica supports have been coated with a solution of TPAOH and immersed in an autoclave containing water (about 3 gr). This method suppresses the change in orientation of the zeolite that is a disadvantage in the traditional hydrothermal synthesis and, at the same time, avoids different steps [47].

The use of microwave instead of conventional heating permits to reduce synthesis time and production cost, a very narrow crystal size distribution, and the reduction of defects [48-50]. Recently, a LTA zeolite membrane has been prepared on the surface of macroporous $\alpha$-$Al_2O_3$ support quite rough and with some significant defects [51]. The seeded alumina support has been grown by microwave for 30 min at 100 °C. The NaA zeolite membrane showed stable water flux (8.24 $kgm^{-2}h^{-1}$) and a rejection of 99.9% by using a 3.5 wt% of NaCl solution. Chew and coworkers have prepared SAPO-34 zeolite membrane with a thickness of 4 μm by microwave heating in 2 h of synthesis. This membrane showed $CO_2$ permeance of $5.8 \times 10^{-7} mol(m^{-2}s^{-1}Pa^{-1})$ and a

$CO_2/CH_4$ selectivity of 30 [52]. In this study, the influence of the cation types in the membrane structure on the gas permeance and selectivity has been also evaluated. The better result has been obtained with the Ba-SAPO-34 membrane capable to exhibit a $CO_2$ permeance of $37.6 \times 10^{-8}$molm$^{-2}$s$^{-1}$Pa$^{-1}$ and a $CO_2/CH_4$ selectivity of 103 with an equimolar feed mixture at 30 °C and 1 bar.

Zeolite membranes with different topologies with microwave heating have been synthesized [53-56].

However, the microwave heating commercial application is complicated for the high cost of the microwave system [57]. Lately, Okubo and coworkers have produced different zeolites (SSZ-13, $AlPO_4$-5, and ZSM-5) using a bath oil heating in a continuous mode during the growth step [58-60]. The oil bath heating seems to possess a similar heating rate to the microwave and so favors the zeolite crystal formation in a short time (enhanced nucleation and crystallization), but it is cheap and so could be an effective alternative to the microwave system. In 2017, for the first time, a SAPO-34 zeolite membrane with oil-bath heating has been fabricated. This membrane has been prepared by secondary growth method and using the rubbing during the seeding step. After the seeding step, the seeded support was soaked in a gel for almost 3 hrs at room temperature. Subsequently, the autoclave has been kept in an oil bath (T = 220 °C). The synthesis time and the membrane thickness have been significantly reduced [61]. The membrane prepared with a synthesis time of 1 hr was very thin (thickness ~ 0.8 μm) and displayed a decent separation performance for $CO_2$-$CH_4$ gas pair ($CO_2$ permeance of $7.5 \times 10^{-7}$mol(m$^{-2}$s$^{-1}$Pa$^{-1}$) and $CO_2/CH_4$ selectivity of 17). The oil-bath heating method has also been employed to synthesize SSZ-13 zeolite membrane [62], even if the synthesis of zeolite membranes with other topologies to be applied in different separation processes is required for its application at the industrial level.

During the years, some research groups have prepared membranes with oriented crystals for improving the molecular sieving effect. For example, Tsapatsis and coworkers synthesized, utilizing the secondary growth method, highly oriented MFI zeolite membranes using a new structural directing agent (a trimer of TPAOH) [63]. These membranes exhibited interesting performance for separating mixtures of chemical species with similar size and shape, such as xylene isomers. However, the new structure-directing agent (SDA) is expensive and difficult to synthesize. Yoon et al. have used tetraethylammonium hydroxide (TEAOH) and $(NH_4)_2SiF_6$, as structural directing agents for the synthesis of b-oriented MFI zeolite membranes [64]. Zhou and coworkers have synthesized a b-oriented silicalite membrane on alumina support and using as reagents TPAOH/tetraethoxysilane (TEOS)/$H_2O$/hydrofluoric acid (HF) [65]. The membrane showed exciting results in the purification of hydrogen produced by steam reforming ($CO_2/H_2$ separation selectivity of 109 and $CO_2$ permeance of $51 \times 10^{-7}$mol m$^{-2}$ s$^{-1}$ Pa$^{-1}$ at 35 °C). Nevertheless, the hydrofluoric acid is very corrosive by limiting the choice of the support type to be used. Wang and coworkers have developed a new synthesis solution composed of tetrapropylammonium bromide (TPABr)/fumed silica/$H_2O$ without HF and have produced highly b-oriented MFI zeolite layers on glass-plate support [66]. Recently, Zhou and coworkers have synthesized highly (h0h)-oriented tubular silicalite-1 membranes by secondary growth method [67]. The prepared membranes have been utilized for separating the butane isomers, and an n-butane/i-butane separation of 36 and n-butane permeance of $25.8 \times 10^{-8}$ mol m$^{-2}$ s$^{-1}$ Pa$^{-1}$ have been obtained. However, the preparation of oriented membranes on a large scale is still critical since a simple, environmentally friendly, scalable, and economical process is required.

Another route explored for reducing the defects is using very thin zeolite nanosheets during the seeding step. Initially, zeolite nanosheets are prepared using a multi-step approach based on the exfoliation of layered MFI [68]. This method is very long, expensive, and with a low yield. Alternatively, a direct synthesis permits the production of zeolite nanosheets with improved yield and at lower cost [69]. The membranes have exhibited impressive performance (very high flux and rejection values) in the desalination process of brine [69]. Zeolite membranes prepared with the nanosheets show mesmerizing performance in terms of permeance and separation, but the preparation process is hard to achieve in terms of feasibility and scalability. Besides, the synthesis is only possible on the Stçber silica-derived disk-type supports that are very difficult to fabricate in tubular or hollow fiber configurations. Recently, Nair and coworkers prepared membranes with nanosheets on macroporous alumina hollow-fibers (HFs) [70]. Uniform 2D nanosheet films were obtained by vacuum filtration on the HFs, and the zeolite layer have been grown by Successively, two sequential hydrothermal treatments. The MFI zeolite membranes have showed high performance for the butane isomer separation (n-butane permeance of $382 \pm 100$ GPU n -butane/i-butane mixture separation factor of 42 at 25 °C).

After the synthesis, the zeolite membranes are calcined for SDA removal. However, this thermal process can determine the formation of pinholes and cracks into the zeolite layer owing to the different thermal expansion coefficients of support and zeolite. A possible way to follow could be the free-template synthesis of the membranes. Liu *et al.* synthesized LTA zeolite membranes enriched in Si by using the template-free secondary growth method [71]. The prepared membranes in pervaporation process achieved interesting water selectivity values (>100,000) for 90–10% of water–ethanol and water-isopropanol mixtures. These membranes were stable for almost 170 h under water-rich conditions (see Fig. 1).

Tsapatsis and coworkers improved the separation performance of the zeolite membranes by reducing the grain boundary defects by a calcination process called “rapid thermal processing” (RTP) [72]. The calcination is usually carried out in the temperature range 400 °C–550 °C for several hours. In the RTP, the membrane is heated up to 700 °C (using an infrared lamp-based furnace) for a minute and then cooled by water circulation. These membranes exhibited better performance than those traditionally calcined. The researchers have hypothesized a condensation of Si-OH groups between adjacent crystals during the new thermal process [72]. Recently, Chang and coworkers have optimized the template removal for the SAPO-34 zeolite membranes [73]. They combined the RTP with the conventional calcination process. The authors used the RTP at 700 °C for 1 min and a fast cooling at 400 °C; subsequently, traditional calcination was performed for 4 hrs followed by slow cooling to room temperature. The membrane has showed a $CO_2$ permeance of $6.1 \times 10^{-7}$ molim$^{-2}$s$^{-1}$Pa$^{-1}$ and a $CO_2/CH_4$ selectivity of 88. The Robeson plot, illustrated in Fig. 2, for $CO_2$–$CH_4$ separation indicated as the optimized calcination process improved the SAPO-34 zeolite membrane performance.

Different post-synthesis techniques for reducing the defects present in the zeolite layer are used. For example, chemical vapor deposition (CVD) of silane compounds (usually tetraethoxysilane) enables to plug of nanometer-scale defects, but it is inefficient for big defects because a large quantity of silane compounds is required [74]. Yang and coworkers prepared deca-dodecasil 3R (DDR) zeolite membranes using the secondary growth method, and CVD for repairing defects (produced during the calcination step) [75]. A membrane performance improvement of the gas separation process has been achieved, as shown in Fig. 3.

Recently, the possibility of curing defects of ZSM-5 membranes using CVD and n-hexane as carbon-source has been investigated [76]. The gas permeation tests evidenced as the gas permeances decreased, the He/$SF_6$ and $H_2/SF_6$ selectivities enhanced with increasing treatment time and using n-hexane as carbon source. The defects are also cured with the coke deposition using liquid hydrocarbons, and two approaches are considered. In the first one, liquid hydrocarbons are larger than the zeolite pores, and the crystalline zeolite pores are not plugged. In the second one, hydrocarbons smaller than the zeolite pores reduce zeolite and non-zeolite pore sizes [77]. Gavalas and coworkers cured defects of ZSM-5 membrane (pore size of about 5.5 Å) with a post-synthetic coking process using a large molecule (1,3,5-triisopropylbenzene; kinetic diameter 8.4 Å). The thermal treatment at 500 °C has been carried out at two different times (2 and 30 h) with coke formation into the defects.

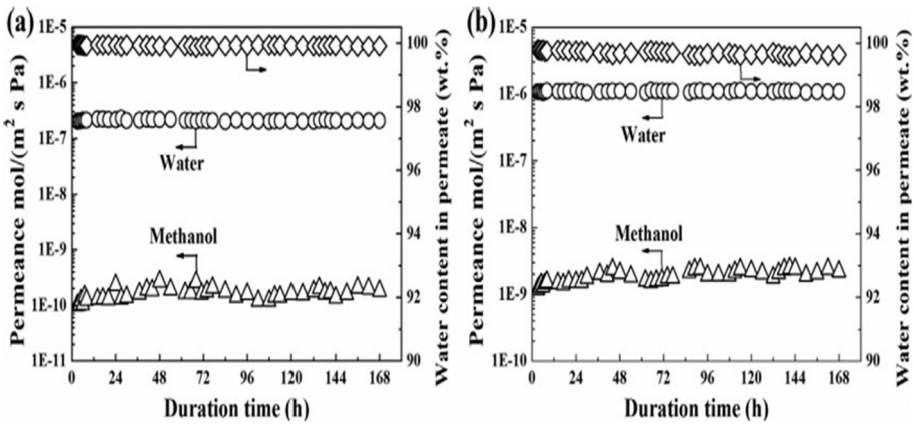


**Fig. 1.** Long-term stability of (a) LTA zeolite membrane (sample: M11-1; Operating conditions: equimolar water-methanol solution at 60 °C for one week), and (b) LTA zeolite membrane (sample: M11-2; Operating conditions: equimolar water-methanol mixture at 150 °C for one week) [71]. Reproduced with permission of Elsevier. B.V. (2021).

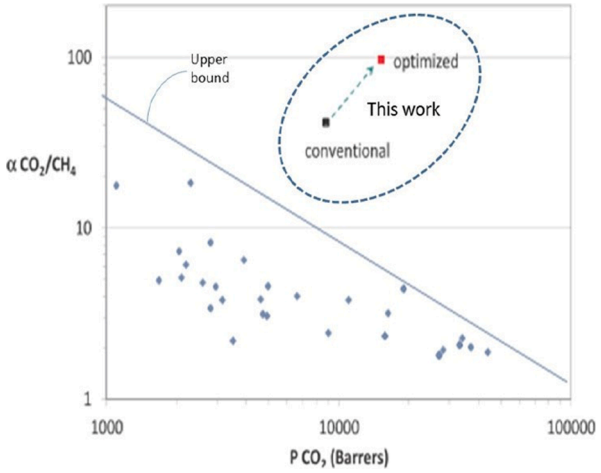


**Fig. 2.** Robeson plot for $CO_2$–$CH_4$ separation. [73]. Reproduced with permission of Elsevier. B.V. (2021).

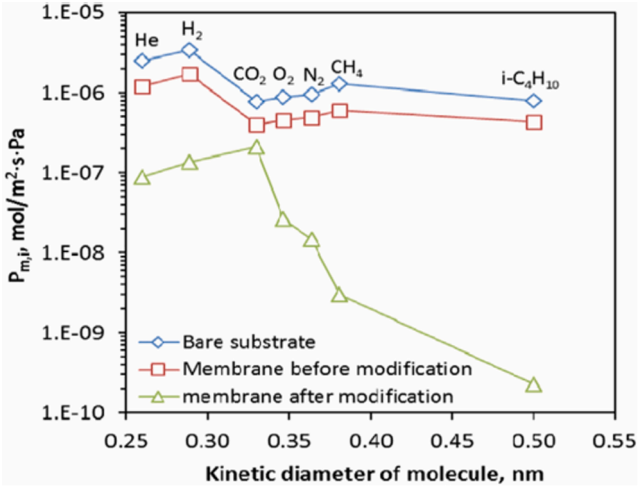


**Fig. 3.** Permeance of gas species as a function of their molecular kinetic diameter for Bare support, zeolite membrane unmodified and modified [75]. Reproduced with permission of Elsevier. B.V. (2021).

The membrane treated for a prolonged time exhibited for the butane isomers very high selectivity (322 at 185 °C) [78]. SAPO-34 zeolite membranes have also been cured by coking treatment by using the methanol to olefin reaction and exploiting the catalytic activity of this zeolite [79]. The surface hydrophilicity of non-zeolitic pores has suffered a weakening owing to the coke deposition. The SAPO-34 zeolite membrane showed a high separation factor (>3200) for the water- 2-propanol (IPA) mixture in vapor permeation. The cured membranes showed a reduced separation factor (170). These results evidenced as the water molecules pass through zeolitic and non-zeolitic pores in the SAPO-34 zeolite membranes, and the size and hydrophilicity of non-zeolitic pores are important factors for inhibiting the IPA permeation.

Sol-gel or a polymeric solution can also cover used for plugging the defects of the membranes [77]. Usually, polymers characterized by higher permeance than the zeolite membrane but lower than the meso and macro-defects are used (e.g., silicon rubbers, mainly polydimethylsiloxane (PDMS)) [80]. In this procedure, it is essential to check the thickness of the polymeric layer deposited on the membrane to ensure high values of both permeance and selectivity. Mu and coworkers repaired the defects of SAPO-34 zeolite membranes with this procedure [81]. The membrane surface has been coated with an organosilica polymer sol by using the vacuum assisted deposition (VAD) and repeating it up to 6 times, and the effect of the treatment on the membrane is shown in Fig. 4.

It is possible to observe, as only one treatment did not cover all the defects. On the other hand, repeated the treatment six times, complete coverage of the zeolite crystals has been observed. The $CO_2$ permeance decreased while the $CO_2/CH_4$ separation factor raised with the number of treatments. The deposition of a silicon rubber solution on the surface of an SSZ-13 zeolite membrane was also performed [82]. The cured membrane presented reduced $CO_2$ permeance and increased $CO_2/CH_4$ selectivity for an equimolar gas mixture at 25 °C and a feed pressure of 2 bar. The polymeric layer on the membrane surface has exhibited resistance to water vapor at 105 °C and several organic solutions.

During the last few decades, a great deal of work has been focused on the development of defect-free zeolite membranes. In spite of the high expectations, there is still a long way to go for the production on a large scale of this type of membranes. Fig. 5 summarizes the successes in the preparation field starting from the one-step method up to the secondary growth method coupled with the oil-bath heating. The secondary growth, as mentioned before, is more reproducible than the one-step method. In addition, the oil-bath heating reduces the synthesis time and membrane thickness, and by minimizing the thermal lag associated with regular oven heating, which facilitates nucleation and crystallization. However, a large-scale application of the zeolite membranes could be possible by using the secondary growth method ultrafast (oil-bath

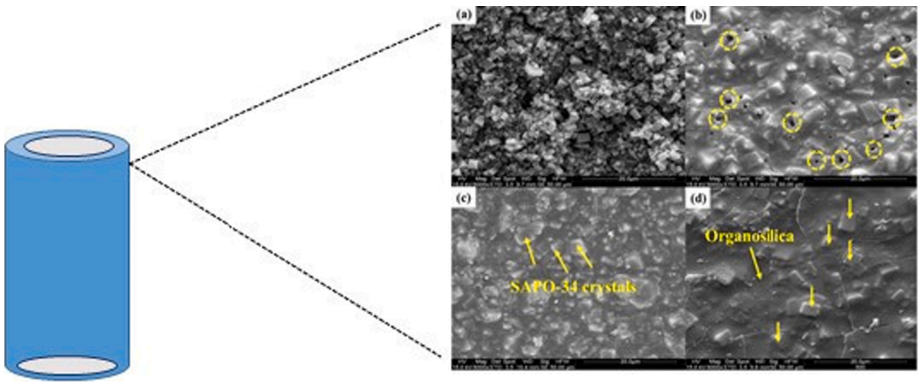


**Fig. 4.** Top-view of (a) un-modified SAPO-34, (b) VAD-OS-1-SAPO-34, (c) VAD-OS-3-SAPO-34, and (d) VAD-OS-6-SAPO-34 zeolite membranes. [Adapted from reference 81].

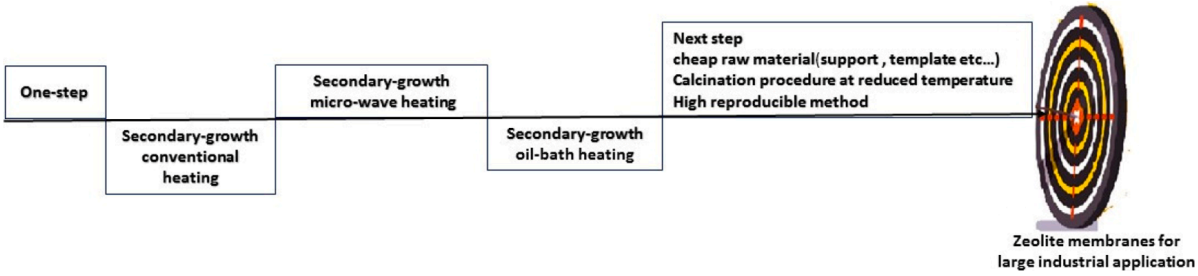


**Fig. 5.** Successes and future trends in zeolite membrane preparation field.

heating) and at the same time using cheap-raw materials (lowering of costs) and calcination procedure fast and performed at low temperatures (costs and the defect formation reduction).

## 3. Zeolite membranes in pervaporation

The demands for organic solvents are growing due to the rapid industrial growth. The dehydration of the organic solvents is significant for their high efficiency. However, many organic water-solvent mixtures form azeotropes. Traditionally, distillation is used but is ineffective when the azeotropic point is reached [83]. Other techniques are used for overcoming the limits of the traditional distillation; however, they are energy-intensive and cause environmental pollution [83]. Pervaporation is a membrane process recognized as a potential candidate instead of the distillation one. In this process, the liquid mixture is in contact with the selective layer of the membrane, and the permeate (in the vapor phase) is collected to the other membrane side. The species with a higher chemical affinity with the membrane are in the permeate stream. For example, a membrane with hydrophilic property must be chosen for the removal of the water from the liquid feed [84].

In this process, the driving force is the vapor pressure difference through the membrane [85], as shown in Fig. 6.

At the lab scale, the vacuum at the permeate site is produced with a vacuum pump, and a dense thin membrane supported on a porous one is usually used for increasing the permeance. The mechanism that describes the transport of the chemical species is the solution-diffusion. The target molecule is adsorbed on the selective layer of the membrane and then diffuses under the action of the driving force [86] (see Fig. 5). The permeability (P) is defined by this equation (1):

$$P = D^{*}S \quad (1)$$

D is a kinetic parameter, S is a thermodynamic parameter of the species adsorbed in the equilibrium condition [85].

The value of P for the specie *i* is calculated using equation (2):

$$P_i = \frac{J_i \bullet l}{\gamma_{i,f} \bullet x_{i,f} \bullet} \bullet (P_{i,f}^{sat} - P_{i,p}) \quad (2)$$

J ($Kgm^{-2}h^{-1}$) is the partial flux of component *i* in the permeate and l (μm) the thickness of the membrane. In addition, $P_{i,p}$ (kPa) is the partial pressure of component *i* in the permeate side (generally assumed to be zero); $\gamma_{i,f}$is the coefficient of activity of the specie *i* in the feed side, and $x_{i,f}$ is the molar fraction of this component in the feed. The $P_{i,f}^{sat}$ (kPa) indicates the saturation vapor pressure obtained utilizing the Antoine equation.

Different hydrophilic membranes are used for the dehydration of organic solvents, and among these the polyvinyl alcohol (PVA) thanks to its high hydrophilicity and abrasion resistance. However, this material is inclined to swelling with reduced selectivity and increased ~~of~~ permeability. Different cross-linkers are used to increase the PVA membrane performance as citric and maleic acid [87] and glutaraldehyde [88,89]. In the pervaporation (PV) process for the solvent dehydration are also employed membranes in cellulose, cellulose acetate and ethyl cellulose and polyamide applied [90-92].

Zeolite membranes showing high chemical resistance with a low degree of swelling represent an exciting alternative to the polymeric ones in PV process [93]. NaA zeolite (LTA topology) membranes are particularly hydrophilic (Si/Al = 1) and with small pores (~0.42 nm)

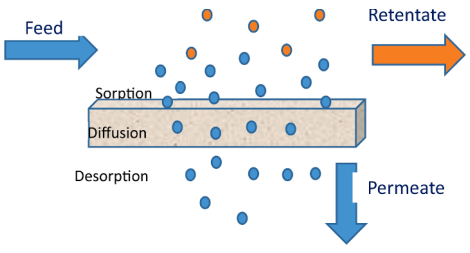


**Fig. 6.** Scheme of a pervaporation membrane process.

and so accessible preferentially to the water molecules and so widely used in the PV process for solvent dehydration. Since the early 1990s, different research groups have focused on the PV process's NaA zeolite membranes preparation and application. In 1999, the first NaA zeolite membrane PV plant was used to dehydrate various organic solvents and was installed in Japan [94]. Today, different companies as Nano-Research Institute Inc. (BNRI), a subsidiary of Mitsui, the European alliance between Smart (UK) and Inocermic, Nanjing Jiusi Hi-Tech Co., and Hitachi Zosen Corporation commercialized zeolite membranes for organics dehydration employing PV process [56].

Sommer and Melin evaluated the performance of the hydrophilic zeolite membranes produced by Mitsui Engineering & Shipbuilding Co. for solvent dewatering [95]. The researchers found for the NaA zeolite membranes that the permeate flux increased with the water content in the feed and with the vacuum applied at the permeate side. In addition, the flux also raised exponentially with the temperature. The performance in the PV process of these membranes has been reported in Table 1.

NaA zeolite membranes exhibit low stability in acidic conditions (just below the neutral value of pH) and the membrane contraction [96]. This behavior was due to the high amount of aluminum in the structure (Si/Al = 1). Jamisien and coworkers reported that the cationic exchange between the $Na^+$ and the $H^+$ happens using acidic solutions [97]. The adsorbed proton catalyzed the hydrolysis of the Al-O bond with a consequence collapse of the structure [97]. T-type membranes with a nanopore size of 0.36 nḿ 0.51 nm also displayed good separation performance in the PV process [98-101]. For example, Zhou and coworkers prepared T membranes using the secondary growth method, and their performance has been assessed in the PV process [102]. The prepared membranes showed very high water/IPA separation factor ($H_2O$/IPA = 13,000) with a flux of 2.50 kg $m^{-2}h^{-1}$ using a feed concentration of 10 wt% of water at 75 °C.

A comparison between the PV performance of Mitsui NaA and T zeolite membranes in Table 2 is reported.

NaA zeolite membranes displayed better performance in selectivity and comparable permeate flux values, even if T-type membranes demonstrated high stability in acidic conditions due to the higher Si/Al ratio (3–4) than that of the NaA zeolite [103].

In the zeolite membrane field, better stability and defect reduction of the zeolite layer could be possible by increasing the Si/Al ratio and preparing template-free membranes to avoid the calcination procedure that usually caused defect formation. Considering these aspects, recently, Kita and coworkers fabricated template-free NaA zeolite membranes with higher Si content (Si/Al = 1.5) [71], and their performance was evaluated in the PV process. The Si-rich LTA membranes were hydrothermally stable in a 50% water-methanol solution at 60 °C. In addition, they exhibited thermal stability in contact with an equimolar vapor water-methanol mixture at 150 °C for one week.

Due to their high permeation flux and higher packing densities, the hollow-fiber membranes receive a lot of attention. For example, Wang et al. synthesized T zeolite membranes on yttria-stabilized zirconia hollow fibers by secondary growth method and using different seeding procedures [104]. The membranes prepared using rubbing displayed a water flux of 7.36 kg $m^{-2}h^{-1}$ with a separation factor over 10,000 using an IPA-water solution (90 wt%–10 wt%) at 75 °C. The use of HFs as support significantly contributes to obtaining very high flux. In any case, optimizing the configuration of hollow fiber membrane modules is very important for further improving the PV performance. Gu and coworkers designed hollow-fiber T-type zeolite membrane modules with different geometric configurations (see Fig. 7), and their performance was evaluated in the PV process for ethanol dehydration [105].

The water flux increased with the temperature for all three-membrane modules; even if the water flux increased by almost 20% and 25% for modules B and C compared with module A at 70 °C. The improvement is due to the optimized geometry of the modules that suppresses the concentration polarization phenomenon because they favor uniform velocity distributions [106,107]. These data show as the separation efficiency is heavily influenced by the geometric configuration of the membrane modules [106].

Some researchers of the Mitsubishi Chemical Corporation used Chabazite (CHA)-zeolite membranes in PV process. They synthesized high-silica (Si/Al = 8) CHA-type membranes on tubular alumina supports having a length of 40 cm [108]. This zeolite membrane presents a small pore size (0.38 × 0.38 nm) and hydrophilic character and so can exert separation through a coupled action of molecular sieving and selective adsorption. The dehydration test was performed using a batch of 44 kg of hydrous n-methylpyrrolidone (NMP) (30 wt% of $H_2O$ and 70 wt % of NMP) and a membrane module containing 31 membranes (area = 0.42 $m^2$). The amount of water in the anhydrous NMP was equal to 0.5 wt% operating at 110 °C .

Mobil-Type Five (MFI) zeolite membranes are studied in different separation processes due to their pore size of about 0.5 nm and good chemical stability [109,110]. Silicalite membranes show a substantial hydrophobic property so that they can separate water from organic solvents in the PV process [111]. However, MFI zeolite membranes prepared on supports as alumina or mullite determine decreased Si/Al ratio due to the support leaching during the hydrothermal treatment [112]. Lin and coworkers prepared MFI zeolite hollow fiber membranes by a modified secondary growth method to minimize the defects and aluminum leaching. It consists of a dual-layer seeding (by dip-coating)

**Table 1**
NaA zeolite membrane (Mistui) performance in PV process [adapted from 95].

| Solvent | Feed water (wt%) | T (°C) | Flux (kgm$^{-2}$h$^{-1}$) | α (–) |
|---|---|---|---|---|
| Methanol | 10 | 60 | 0.46 | 10.000 |
| Ethanol | 10 | 70 | 1.12 | 18.000 |
| IPA | 10 | 75 | 1.58 | 30.000 |
| n-Butanol | 9.9 | 75 | 1.40 | 90.000 |
| Ethylene Glycol | 9.3 | 100 | 0.03 | 162.000 |
| Phenol | 8.2 | 100 | 4.69 | 9.400 |
| Acetone | 12 | 53 | 1.12 | 1.500 |
| Acetonitrile | 9.0 | 72 | 2.54 | 1.400 |
| Dimethylacetamide | 10.5 | 80 | 1.51 | 1.600 |
| dimethyl formamide | 9.1 | 82 | 1.51 | 2.400 |
| Tetrahydrofuran | 10.4 | 60 | 1.78 | 12.000 |

**Table 2**
NaA and T zeolite membranes (produced by Mitsui) performance in PV process [Adapted from 95].

| Solvent | Feed water (%) | T (°C) | Flux (kgm$^{-2}$h$^{-1}$) | | α (–) | |
|---|---|---|---|---|---|---|
| | | | NaA (Mitsui) | T (Mitsui) | NaA (Mitsui) | T (Mitsui) |
| Methanol | 10 | 60 | 0.46 | 0.27 | 10,000 | 100 |
| Ethanol | 10 | 70 | 1.12 | 0.91 | 18,000 | 1000 |
| IPA | 10 | 75 | 1.58 | 2.10 | 30,000 | 9000 |
| n-Butanol | 9.9 | 75 | 1.40 | 1.70 | 90,000 | 18,000 |
| Ethylene Glycol | 9.3 | 100 | 0.03 | 0.06 | 162,000 | 150,000 |

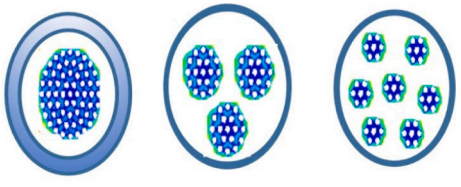


**Fig. 7.** Section of the different modules. [Adapted from Ref. 105].

and a variable temperature during the growth step [113]. The idea is to use large crystals during the first seeding and cover the defects using small ones during the second one. In addition, the variable temperature favors controlling the nucleation and growth reaction rates. The PV tests have been carried out with an ethanol–water mixture (5 wt% of ethanol) at 25 °C. The better results in terms of separation factors have been obtained with the membrane prepared at low initial temperature (125 °C) during the growth step since in these conditions, small crystals are synthesized, and the defects can be plugged. Table 3 reassumes the synthesis conditions and the performances of membranes prepared in this work [113]. The table also reports the ethanol–water pervaporation results obtained with silicalite membranes prepared by other research groups.

These results evidence as the separation factors are not very high due to the defects into the zeolite layer and the leaching of the aluminum from the support that determines a lowering of the Si/Al ratio (reduction of the hydrophobic character).

Hydrophilic zeolite membranes applied in PV process for the dehydration of solvents as dimethylacetamide (DMA) and dimethyl formamide (DMF)) exhibit low water flux [119,120]. The strong adsorption of the amides (DMA or DMF) with the ionic sites of the zeolite membranes determines a blockage of the water sites and so the water flux reduction. This behavior is due to the higher dipole moment of the amides than the alcohols [120,121]. Gu and coworkers have modified the surface of hollow fibers NaA zeolite membranes with sol–gel derived $TiO_2$ to improve their performance for the DMA dehydration in the PV process [121]. $TiO_2$(0.5)/NaA zeolite membrane has been entirely covered by the $TiO_2$ layer chemically bounded with the cations species ($Na^+$). Therefore, the electrostatic interaction between cations and DMA molecules has been hindered. This layer also supplies a low transfer resistance for water that easily passes through the membrane. The membrane showed a water flux of 4.66 and a separation factor of 2120 at 90 °C. However, increasing further the $TiO_2$ content (samples $TiO_2$(0.75)/NaA zeolite and $TiO_2$(1.0)/NaA zeolite membranes) not only the interaction with the amide but also the water flux has been strongly reduced.

In Fig. 8 is illustrated the separation factor versus the permeate flux for the ethanol–water separation of different zeolite membranes (the PV experiments have been performed in the same operating conditions: T = 70–75 °C; 90 wt% ethanol and 10 wt% of water).

Many papers are published on the organic solvents dehydration by using different zeolite membrane topologies, even if NaA zeolite membrane has exhibited better performance in terms of separation and water flux. This zeolite topology for the small pore diameter and the high hydrophilicity permits the preferential adsorption of the water molecules, and the alcohol molecules cannot permeate through the membrane.

The results analyzed in this section highlight the significant progress made in this field for improving flux, separation factor, and stability. However, their reduced application at an industrial scale depends on the lack of process technology for membrane manufacturing with high reproducibility and defect-free.

**Table 3**
Silicalite membrane performance in $N_2/SF_6$ and ethanol/water separations [adapted from 113] and comparison with literature data.

| Sample | Single-layer | growth step temperature, (°C); (Time) | Method for Synthesis | $N_2/SF_6$ ideal selectivity (–) | PV test | Total fux (kg $m^{-2}h^{-1}$) | Water /Ethanol separation factor (–) | Ref. |
|---|---|---|---|---|---|---|---|---|
| M1 | 1500 | 175 | Secondary | 2.52 | Ethanol (5 wt%) | – | – | [113] |
| M2 | 600 | | Growth | 3.36 | T = 25 °C | 2 | 22 | |
| M3 | 100 | | | 8.48 | | – | – | |
| | | | | | | | – | |
| | Duable-layer (top/bottom) | | | | | | | |
| M4 | 1500/1500 | 175 | | 6.30 | Ethanol (5 wt%) | – | – | |
| M5 | 1000/1500 | | Secondary | 21.7 | T = 25 °C | – | – | [113] |
| M6 | 600/1500 | | Growth | 37.8 | | – | – | |
| M7 | 400/1500 | | | 41.2 | | 22 | 46 | |
| M8 | 100/1500 | | | 57.2 | | 6.8 | 66 | |
| | | | | | | – | – | |
| | Duable-layer (top/bottom) | | | | | | | |
| M9 | 100/1000 | 175 | Secondary | 120.4 | Ethanol (5 wt%) | 4.7 | 66 | [113] |
| M10 | 100/600 | | Growth | 173.5 | T = 25 °C | 2.3 | 101 | |
| M11 | 100/400 | | | 192.5 | | 1.5 | 128 | |
| M12 | 100/100 | | | 203 | | – | – | |
| M13 | 100/600 | 125 (4 h)—175 (4 h) | Secondary | 103.5 | Ethanol (5 wt%) | – | – | [113] |
| M14 | | 125 (3 h)—2h—175 (3 h) | Growth | 162.2 | T = 25 °C | 2.9 | 160 | |
| M15 | | 175 (3 h)—2h—125 (3 h) | | 94.8 | | 3.9 | 95 | |
| M16 | | 175 (4 h)—125 (4 h) | | 124.1 | | – | – | |
| Silcalite (a)* | – | 175 (144 h) | One Step | – | Ethanol (5 wt%) T = 30 °C | 0.15 | 51 | [114] |
| Silcalite (a)** | – | 175 (144 h) | One Step | – | Ethanol (5 wt%) T = 30 °C | 0.14 | 125 | [114] |
| Silicalite | – | 175 (16 h) | One Step | – | Ethanol (5 wt%) T = 60 °C | 0.93 | 96 | [115] |
| Silicalite | Single seeding | –175 (4 h) | Secondary growth | – | Ethanol (5 wt%) T = 60 °C | 1.82 | 62 | [116] |
| Silicalite | Single Seeding | 175 (4 h) | Secondary growth | | Ethanol (5 wt%) T = 60 °C | 1.89 | 64 | [117] |
| Silicalite | Single Seeding | 175 (12 h) | Secondary growth | | Ethanol (5 wt%) T = 60 °C | 9.80 | 58 | [118] |

*Without curing treatment with PDMS.
*With curing treatment with PDMS (3 wt%).

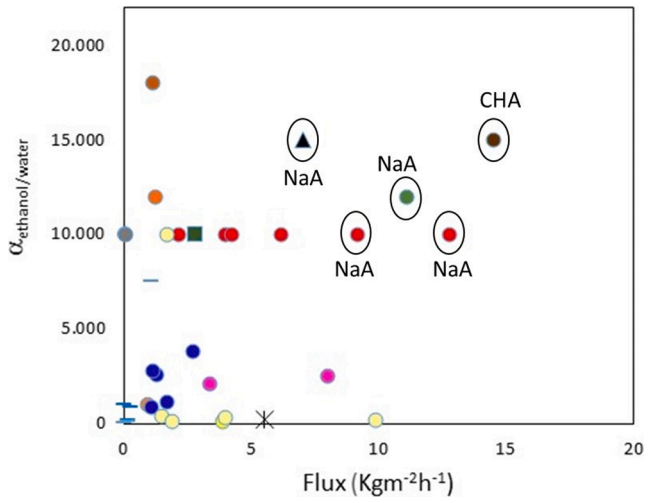


**Fig. 8.** Ethanol-water separation factor versus water flux for different zeolite membranes. Orange Circle: NaA zeolite membrane [95]; Violet Circle: T zeolite membrane [122]; Green square: NaA zeolite membrane [123]; Black Circle: NaA zeolite membrane [124]; Red Circle: NaA zeolite membrane [125]; Blue Circle: T zeolite membrane [126]; Brown Circle: CHA zeolite membrane [127]; Yellow Circle: NaX zeolite membrane [128]; Orange Circle: T zeolite membrane [129]; Black Triangle: NaA zeolite membrane [130]; Black Star: NaX zeolite membrane [131]; Blue dash: Mordenite zeolite membrane [132]. (For interpretation of the references to color in this figure legend, the reader is referred to the web version of this article.)

## 4. Zeolite membranes in desalination

The fresh water for the earth's population is minimal, and in 2025 the fifty percent of it will face a water shortage [133]. The desalination process represents a water shortage solution because 97.5% of the earth is salt water. Traditionally, thermal distillation has been used for saline water desalination, but it is costly for both energy required for water heating and high costs of plant maintenance [134]. An alternative route is represented by reverse osmosis (RO), a pressure-driven membrane process, which allows ~~for providing~~ to provide clean water for drinking, industries, and agriculture [135]. This process offers various advantages as reduced energy usage associated with the employment of low-cost construction materials, high quality of water, and elevated efficiency [136]. Today, the RO dominates the desalination market [137] and the most of desalination plants (seventy percent) are located in the Middle East [138,139].

Most of the membranes used in RO are polymeric ones due to their low cost, simple manufacturing, and easy processability. Critical issues in the polymeric membrane field are the fouling responsible for several adverse effects as deterioration of water quality, reduced membrane lifetime [140], and the trade-off between permeability and selectivity [3]. For reducing the fouling effect, the membranes are continuously washed with chemical solutions to ensure elevated flux and selectivity. Feed pretreatment is also performed (e.g., microfiltration/ultrafiltration processes) to minimize fouling [141]. Zeolite membranes, for their nanoporous structure, are capable of removing ions from saline water and thus suitable for carrying out the desalination process. Several years ago, Li and coworkers used silicalite zeolite membranes, prepared on alumina disk support with the one-step method, in the RO desalination process [142]. The authors obtained a flux of 0.112 kg $m^{-2}h^{-1}$ and a salt rejection of 76.7% by using as feed a sodium chloride solution (0.1 M) [142]. They also stated that water flux and ion rejection are influenced by the size, diffusivity, and ion charge [143]. The experimental data also evidenced as a different mechanism regulated the ion rejection through zeolite pores and inter-crystalline defects. Ion rejection on the zeolite channels is controlled by a size exclusion effect on the large hydrated ions. Ion separation through the defects is due to the strong interaction between the ion and the charged double layer, and the ion diffusion through the microporous space is reduced [143].

The influence of the Si/Al ratio of different MFI zeolite supported membranes on the RO performance was also evaluated [144]. It has been found an improvement of flux and rejection with an increase of the Al content due to the high surface charge of the zeolite layer and a better affinity with water molecules. Silicalite zeolite membrane (hydrophobic character) showed a rejection of 90.6% and a water flux of 0.112 $kgm^{-2}h^{-1}$. Furthermore, the presence of the aluminum species (low concentration) in the zeolite structure determined an increase of both water flux (1.129 $kgm^{-2}h^{-1}$) and ion rejection (92.9%). When the Al content increased, the ion rejection decreased (81.8%), explained by the enlarged intercrystalline pores and poor zeolite crystallinity [145]. Same results have been found by Duke and coworkers [146].

NaA zeolite membranes having a length of 40 cm (area: 90 $cm^2$) have been employed in water desalination by using the PV process, and seawater from Boryeong Beach on the West Seacoast of South Korea as feed [147]; the water flux and the rejection were of 1.9 $kgm^{-2}h^{-1}$, and 99.9% (for all the ions), respectively. The high flux value is explained by the electrostatic interaction between the surface charge of the membrane and the water a polar molecule. In addition, the high rejection is due to the charge exclusion mechanism because the positive charge (metal cations adsorbed on the membrane surface) that prevents hydrated cations from passing through the zeolitic pores.

Silicalite and ZSM-5 membranes, prepared by secondary growth method on tubular alumina support (5 cm long), have been used for long-term desalination of salty (NaCl) solution at different concentrations and using a PV lab plant [148]. The experimental data are shown in Fig. 9. The two membranes have exhibited comparable performance using a seawater salt concentration (3.5 wt%) and varying the temperature from 21 °C to 75 °C (see Fig. 9a). Using a brine solution (7.5 wt%) a structure degradation of the ZSM-5 membrane has been observed in a time range of about 300 hrs (see Fig. 9). The authors explained the modification of the ZSM-5 structure considering the cation exchange between the zeolite and the $Na^+$ ions [149]. A long-term hydrostability property has been found for the silicate membrane using pure water as feed.

Zhou and coworkers evaluated the desalination performance of MFI zeolite membranes, fabricated with the secondary growth method and the rubbing as seeding procedure, by using saline recycled wastewater in the RO process [150]. Rejection of 80% and flux of 4.0 $Lm^{-2}h^{-1}$ have been obtained operating at a pressure difference of 70 bar. The authors have also studied the effect of chlorine for removing biofouling since it has a harmful impact on commercial RO membranes. The membrane resisted under chlorine exposure indicating its high chemical resistance and so enabling the biofouling control.

Tubular silicalite membranes (length of 30 cm) have been characterized for water desalination in the vacuum membrane distillation process [34,35]. The tests have been performed at 60 °C, with a feed flow rate of 75 $Lh^{-1}$ and using different NaCl solution concentrations (0.2, 0.6, 0.9, and 1.2 M). Moving from 0.2 M to 0.9 M, the rejection values have been high and almost constant (>99.5%), but at the same time, an increase in the sodium chloride concentration has determined a decrease in the water flux [35]. Using brine solution (1.2 M), a decrease in water flux and rejection has been detected, owing to the higher amount of salt entrapped and accumulated on the membrane surface (feed side) by inducing the concentration polarization [151]. A water activity decrease is also verified to decrease the water mole fraction in the solution with a decline of the driving force [152]. The same authors have demonstrated the possibility to improve the VMD performance for water desalination by using MFI zeolite membranes [153] (prepared as already done in their previous works) [34,35]. In particular, operating at 70 °C and a feed flow rate of 120 $Lh^{-1}$ and in the salt concentration range of 0.2 M–0.9 M, the rejections remained almost constant (~99.9%) and the permeate flux slightly decreased (from 20.6 $kgm^{-2}h^{-1}$ (0.2 M) to 18.0 $kgm^{-2}h^{-1}$ (0.9 M)). These exciting results

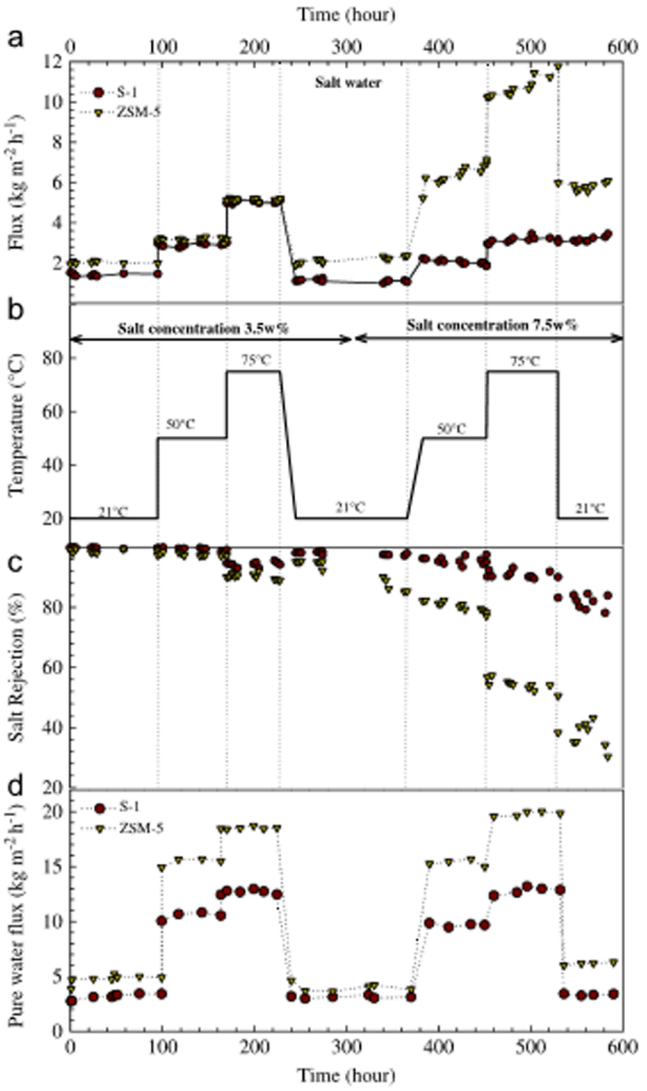


**Fig. 9.** Long term experiments performed of silicalite (S-1, circle) and ZSM-5 (triangle) membranes: (a) water flux (feed: NaCl solution); (b) during thermal cycling, (c) Rejections, and (d) water flux (feed: pure water) [148]. Reproduced with permission of Elsevier. B.V. (2021).

have been explained considering the coupled positive action of feed-flow rate and temperature. An increase in the feed flow rate has permitted removing the salt deposited on the membrane surface. At the same time, a higher temperature has produced an increase in the saturated pressure of water vapor with a rise of the driving force through the membrane (the driving force is the water vapor pressure difference between the feed and permeate sides) [154]. Using as feed a brine a solution (1.2 M), the flux (12.2 kgm$^{-2}$h$^{-1}$) and the rejection (97.13%) have significantly decreased. Nevertheless, a comparison with previous work [35] evidenced improved rejection (97.13% vs. 94.6%) due to the positive effect of the increased feed-flow rate and temperature. After the VMD test on the 1.2 M solution and cleaning procedure, other tests with pure water and salty solutions were carried out, leading to reproducible fluxes and rejections.

Wang et al. have studied water desalination by using zeolite membranes characterized by different topologies (LTA, MFI, AEI) and prepared by secondary growth method on porous stainless-steel-net of 300 mesh (purchased from State No. 540 Co. Ltd. (Xinxiang, China)) [144,155]. The results in terms of water permeability and rejection for various salt solutions at 20 °C in the PV process are reported in Table 4 [155].

The three membranes have exhibited very high ion rejection (>99%), confirming as the zeolite pore regulates the cation removal. In fact, all the cation hydrated diameters are higher than the zeolite pore sizes ($Na^+$=7.16 Å, $K^+$=6.62 Å, $Mg^{2+}$= 8.56 Å and $Ca^{2+}$=8.24 Å; $H_2O$ = 2.76 Å; zeolite pore size (AEI) = 3.8 Å; pore size (LTA) = 4.1 Å; pore size (MFI) = 5.5 Å). In addition, the highest water permeability has been found with the AEI zeolite characterized by a smaller pore size; this trend is due to the electrostatic interaction between the water molecules and the surface charge of the zeolite [147]. In Table 5, the different results discussed in this section are summarized.

Applying the zeolite membranes in the desalination process enables obtaining significant rejection and water flux results when prepared to employ the secondary growth method. Anyway, their application at an industrial scale requires defect-free membranes that still represents a challenge. The inter-crystalline and intra-crystalline defects determine a drastically change of the membrane permeation properties.

## 5. Zeolite membranes in natural gas purification

Polymeric membranes are largely used for low cost and highly reproducible preparation in the gas separation processes [156]. The permeability-selectivity trade-off and other challenges, as plasticization, physical aging, and swelling, limit their performance [157]. Zeolite membranes for their characteristics have been studied in different gas separation processes [158-165]. In this review, attention has been focused on the application of zeolite membranes in natural gas purification.

### 5.1. Natural gas purification

Today, natural gas (NG) is the primary global energy source, and its use will grow by about 1.6–2.0% for the year up to 2040 [165]. The NG main component is methane ($CH_4$) even if other gas species are present, and the composition is reported in Table 6 [166].

The removal of acid gases as $CO_2$ and $H_2S$ is necessary, being very corrosive for the pipelines and with the possibility to cause health problems [167]. Carbon dioxide also determines the heating value lowering of the combustible gas [168]. Today, $CO_2$ removal is mainly achieved using alkanolamines (monoethanolamine, diethanolamine, triethanolamine, methyl diethanolamine, di-isopropanolamine nd diglycolamine) [169]. This process suffers from high operating and maintaining costs. The amines are quite toxic, and a malfunction of the plant can determine a bad impact on humans, animals and the environment [170]. Membrane technology represents a positive alternative

**Table 4**
Permeability of water (P) and rejection (R) for various salt solution for the three zeolite membranes. Ref. [155]. Reproduced with permission of Elsevier. B.V. (2021).

| Feed Solution | Concentration (molL$^{-1}$) | AEI | | LTA | | MFI | |
|---|---|---|---|---|---|---|---|
| | | P mol m$^{-2}$s$^{-1}$Pa$^{-1}$ | R (%) | P mol m$^{-2}$s$^{-1}$Pa$^{-1}$ | R (%) | P mol m$^{-2}$s$^{-1}$Pa$^{-1}$ | R (%) |
| NaCl | | $4.183 \times 10^{-10}$ | 99.86 | $3.473 \times 10^{-11}$ | 99.44 | $2.415 \times 10^{-11}$ | 99.82 |
| $MgCl_2$ | | $2.819 \times 10^{-10}$ | 99.6 | $4.806 \times 10^{-11}$ | 100 | $1.811 \times 10^{-11}$ | 99.97 |
| KCl | | $3.850 \times 10^{-10}$ | 99.94 | $6.006 \times 10^{-11}$ | 100 | $1.967 \times 10^{-11}$ | 99.99 |
| $CaCl_2$ | | $2.902 \times 10^{-10}$ | 99.99 | $5.666 \times 10^{-11}$ | 1000 | $1.382 \times 10^{-11}$ | 99.99 |

**Table 5**
Comparison of zeolite membranes used in water desalination process.

| Sample | Configuration | Length (cm) | Synthesis method | Seeding Procedure | Process | Feed (g/l) | T (° C) | Flux ($Kgm^{-2}h^{-1}$) | R (%) | Ref. |
|---|---|---|---|---|---|---|---|---|---|---|
| ZSM5 (MFI) | Disk | – | One-step | – | RO | 5.8 | 25 | 0.12 | 77 | [105] |
| Silicalite (MFI) | Disk | – | Secondary growth | Dip-coating | RO | 5.8 | 25 | 0.11 | 90.6 | [107] |
| ZSM5 (MFI) | Disk | – | Secondary growth | – | RO | 38 | 70 | 0.55 | 99.0 | [108] |
| NaA (LTA) | Tubular | 40 | Secondary growth | Vacuum | PV | 35 | 69 | 1.9 | 99.9 | [109] |
| Silicalite (MFI) | tubular | 30 | Secondary growth | Cross-flow seeding-coupled with the rotation and tilting of the support | VMD | 35 | 70 | 19.0 | 99.9 | [115] |
| Silicalite (MFI) | Tubular | 5 | Secondary growth | Dip-coating | PV | 35 | 75 | 5.10 | 98 | [110] |
| Silicalite (MFI) | Disk | – | Secondary growth | – | PV | 29 | 25 | 0.37 | 99.82 | [117] |
| ZSM5 (MFI) | Disk | – | Secondary growth | – | PV | 35 | 80 | 1.22 | 99.80 | [117] |
| NaX (FAU) | Tubular | – | One-step | – | PV | 35 | 90 | 5.64 | 99.8 | [119] |
| Silicalite (MFI) | Disk | – | One-step | – | PV | 30 | 75 | - | 93.0 | [120] |

**Table 6**
Compositions of natural gas [adapted from 174].

| Hydrocarbons | Composition Wet (vol%) | Composition Dry (vol%) | Non-hydrocarbons | Composition Wet (vol%) |
|---|---|---|---|---|
| Methane | 84.6 | 96.0 | Carbon Dioxide | < 5 |
| Ethane | 6.4 | 2.00 | Helium | ≤ 0.5 |
| Propane | 5.3 | 0.60 | Hydrogen Sulfide | ≤ 5 |
| Isobutane | 1.2 | 0.18 | Nitrogen | ≤ 10 |
| n-Butane | 1.4 | 0.12 | Argon | ≤ 0.05 |
| Isopentane | 0.4 | 0.14 | Radon | Traces |
| n-Pentane | 0.2 | 0.06 | Krypton | Traces |
| Hexane | 0.4 | 0.10 | Xenon | Traces |
| Hepthane | 0.1 | 0.80 | – | – |

**Table 7**
Topology and pore size of various zeolites used in light gases separation process.

| Zeolite | Topology | Cavity size (nm) | Pore size (nm) | Chemical Composition |
|---|---|---|---|---|
| SSZ-13[a] | CHA[b] | 0.835 | 0.38 × 0.38 | Si, O, Al (High Si); Si/Al > 5 |
| CHA | CHA | 0.835 | 0.38 × 0.38 | Si, O, Al (Low Si) 2 < Si/Al < 3 |
| Si-CHA | CHA | 0.835 | 0.38 × 0.38 | Si, O (pure silica) |
| SAPO-34 | CHA | 0.835 | 0.38 × 0.38 | SI, O, Al, P |
| DD3R[c] (or all-silica-DDR) | DDR | – | 0.44 × 0.36 | Si, O (All silica) |

[a] Standard Oil Synthetic Zeolite-13.
[b] Chabazite.
[c] dodecasil 3R.

to the traditional ones [171]. The first membrane system for $CO_2/CH_4$ separation was introduced in the 1980s by different companies: Grace Membrane Systems (a division of Grace Membrane Systems), Cynara (now part of Natco), and Separex (now part of UOP) [167]. Today, different polymers are used for synthesizing membranes for this gaseous separation-type as polyimide (PI), cellulose acetate (CA), polyethersulfone (PES), polysulfone (PSf), and polycarbonates (PC), though, at the industrial level, are used the first two ones [172]. However, these polymeric materials swell (plasticization phenomenon) with a marked decrease in selectivity under the action of high $CO_2$ pressure. Another disadvantage is represented by the trade-off between permeability and selectivity [173,174]. Therefore, great attention has been devoted to zeolite membranes characterized by small pores as SSZ-13, SAPO-34, DD3R that are suitable for separating small species utilizing both molecular-sieving effect and strong adsorption capacity. The characteristics of these zeolites are reported in Table 7.

For the first time, Falconer and coworkers prepared SSZ-13 (CHA topology) zeolite membranes on stainless steel tubular supports [175]. The ideal selectivities have been significantly higher than the Knudsen ones at 25 °C and 200 °C, and the gas permeances decreased with the kinetic diameter increase. In 2014, Kosinov et al. synthesized SSZ-13 zeolite membranes (with high silica content: in the gel Si/Al = 100) on hollow fiber alumina supports [176]. The separation selectivity and $CO_2$ permeance increased by increasing the $CO_2$ partial pressure because the $CO_2$ is preferentially adsorbed over the other components. The results evidenced as the SSZ-13 zeolite membranes are $CO_2$-selective, and the selectivity is achieved for the stronger adsorption of $CO_2$ and its smaller kinetic diameter than the zeolite pore.

Water vapor in the NG is an impurity removed before its access in the pipeline; its presence determines the corrosion and freezing along the pipelines [177]. Some researchers have studied the effect of humidity on the $CO_2$ permeance by using a pure silica CHA (Si-CHA) membrane [178]. An ideal $CO_2/CH_4$ selectivity of 130 and $CO_2$ permeance of $4.0 \times 10^{-6}$ $molm^{-2}s^{-1}Pa^{-1}$ have been found operating at 20 °C and $P_{feed} = 1$ bar in dry condition. The presence of water molecules has determined a decrease of the $CO_2$ permeance due to the water adsorption into the pores of the zeolite crystals (see Fig. 10) [178]. In addition, the permeance of the carbon dioxide increased by raising the feed pressure for the reduced coverage of water molecules. $CO_2/CH_4$ ideal selectivity in dry and wet conditions, were almost the same (about 30) at a pressure of 6 bar.

The effect of the aluminum content (Si/Al ratio in the gel was varied from 5 to 100) in SSZ-13 zeolite membranes (prepared on hollow fibers by secondary method) for $CO_2$ separation has also been evaluated, and the results are shown in Fig. 11 [179]. A decrease in the aluminum content has determined an increase in the $CO_2/CH_4$ selectivity. The Al determines the development of defects in the zeolite layer because it blocks the zeolitization and the formation of the zeolite layer [26,74]. Anyway, the preparation of membranes with very low amount of aluminum (Si/Al ratio higher than 100) was not possible for the presence of a competing zeolite topology (AFI) that has caused a lowering of the membrane performance.

Zeolite membranes with CHA topology had been prepared using the N,N,N-trimethyl-1-adamantammoniumhydroxide (TMAdaOH) as a template expensive and toxic [180]. Different research groups have prepared CHA membranes by developing simple, economical, and

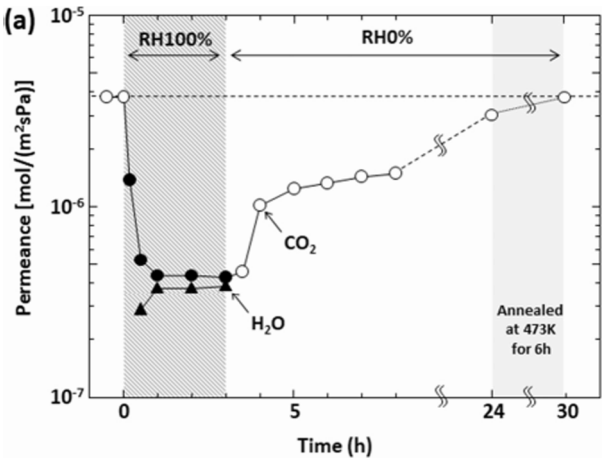


**Fig. 10.** $CO_2$ permeance through a Si-CHA membrane with and without water (operating conditions: T = 25 °C and $P_{feed}$ = 3 bar) [178]. Reproduced with permission of Elsevier. B.V. (2021).

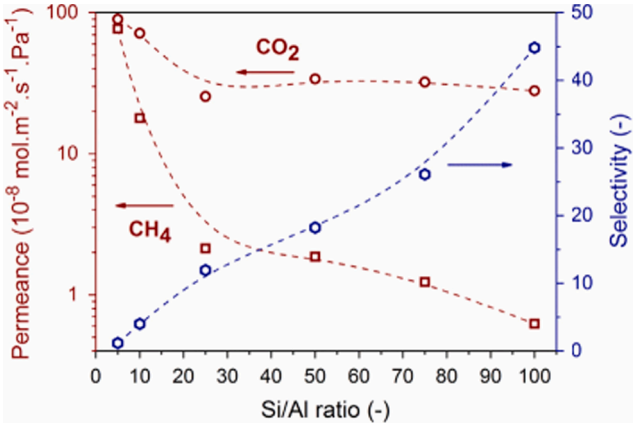


**Fig. 11.** $CO_2/CH_4$ separation versus the Al content in SSZ-13 zeolite membrane. Operating conditions: equimolar $CO_2/CH_4$ mixture, $P_{feed}$ = 6 bar, T = 20 °C [179]. Reproduced with permission of Elsevier. B.V. (2021).

environmentally friendly processes. A high silica CHA membrane has been prepared by using TEAOH as a template [181]. XRD analyses evidenced as small peaks of the CHA-type zeolite after a synthesis time of 12 h. The presence of both FAU and CHA zeolites has been observed with a synthesis time of 24 hrs. Prolonged synthesis time (36 hrs) has favored the formation of the only CHA-type zeolite. These membranes showed $CO_2$ permeance of $3.5 \times 10^{-6}$ mol $m^{-2}s^{-1}Pa^{-1}$ and an ideal $CO_2/CH_4$ selectivity of 90. Hedlund and coworkers synthesized high silica CHA membranes in fluoride media [182] for reducing the defects of the zeolite crystals as described in the literature [183,184]. These membranes, prepared on flat alumina supports, displayed a separation selectivity of 47 and a very high $CO_2$ permeance ($84 \times 10^{-7}$ molm$^{-2}$ $s^{-1}Pa^{-1}$) using an equimolar $CO_2/CH_4$ mixture at 20 °C and with a feed pressure of 9 bar).

Another zeolite used for separating light gases is the SAPO-34, a silicoaluminophosphate material characterized by CHA topology (see Table 7). One of the earliest works on SAPO-34 zeolite membranes supported on alumina disk (prepared by in situ method) has been presented by Lixiong *et al.* [185]. The prepared membranes had been almost defect-free, and exhibited the ability to separate small species by means of the molecular-sieving effect. Falconer and coworkers evaluated the influence of some impurities on permeance and selectivity of $CO_2$ and $CH_4$ by using SAPO-34 zeolite membranes (prepared on stainless steel supports and using the in situ method for the synthesis) [186]. $N_2$ (3%) in $CO_2$-$CH_4$ gas feed had a negligible effect on selectivity and permeance. The presence of 1% of hydrocarbons ($C_2H_4$, $C_3H_8$, and n-$C_4H_{10}$) has determined a lowering of both $CO_2$ permeance and selectivity, and their values decreased more, increasing the hydrocarbons concentration.

In 2008, for the first time, Noble *et al.* [187] prepared SAPO-34 zeolite membrane by using the secondary growth method. The prepared membranes exhibited high reproducibility and exciting performance for the $CO_2/CH_4$ separation. Subsequently, the same research group scaled up (from 5 cm to 25 cm in length) SAPO-34 zeolite membranes on stainless steel tubes. The effect of aluminum sources, gel compositions, separation performance, and membrane cost has also been investigated [188]. Membranes with selectivities of about 250 have been synthesized by increasing the $H_2O/Al_2O_3$ ratio from 77 to 150 (in the synthesis gel). A water content increase has raised the linear growth rate of the crystals and so the reduction of the defects in the zeolite layer. Using cheaper Al-source $Al(OH)_3$ (instead of $Al(i\text{-}C_3H_7O)_3$) has allowed the preparation of reproducible membranes and without loss in permeance and selectivity.

Seven years later, for the first time, a research group from the Nanjing Tech University prepared SAPO-34 zeolite membranes on alumina four-channel hollow fiber supports [189]. The membranes have been synthesized with the secondary method and using the dip-coating during the seeding step. The membranes prepared with small crystals (of about 300 nm during the dip-coating) and treated hydrothermally at 180 °C for 18 h presented interesting perm-selective properties ($CO_2$ permeance of $1.18 \times 10^{-6}$ mol $m^{-2}s^{-1}Pa^{-1}$ with a $CO_2/CH_4$ selectivity of 160). The presence of moisture determined a lowering of the membrane performance due to water's high affinity with the SAPO-34 zeolite membranes. The SAPO-34 zeolite membranes are unstable under the effect of the water vapor that induces changes of the Si-O-Al bonds with the crack formation in the zeolite structure [190].

Gu and coworkers cured SAPO-34 zeolite membranes with PDMS solutions (at different polymer concentrations) by dip-coating [191]. The use of PDMS solutions for curing membrane defects and also for modifying the membrane surface from hydrophilic to hydrophobic is deeply reported in the literature [192,193]. The cured and no-cured zeolite membranes have been characterized in $CO_2/CH_4$ separation process utilizing an equimolar mixture in dry and wet conditions at 25 °C, and the results are reported in Table 8.

The PDMS has cured the defects and reduced the affinity of the membrane with the water. Excellent separation performance for $CO_2/CH_4$ mixtures in dry and wet conditions has been obtained with a concentration of the PDMS solution of 7.5 wt%. In addition, this membrane has shown a stable performance after half-year (only 5–8% change in $CO_2$ permeance and $CO_2/CH_4$ selectivity has been detected). A higher PDMS concertation has reduced both permeance and selectivity for the plugging of non-zeolite and zeolite pores.

**Table 8**
Performance of SAPO-34 zeolite membranes in $CO_2/CH_4$ separation before and after PDMS treatment. Reprinted from [191]. (With permission of Elsevier).

| Water Vapor (%) | No-cured Membranes | | Cured Membranes PDMS (6.5%) | |
|---|---|---|---|---|
| | $CO_2$ permeance mol $m^{-2}s^{-1}Pa^{-1}$ | $CO_2/CH_4$ (–) | $CO_2$ permeance mol $m^{-2}s^{-1}Pa^{-1}$ | $CO_2/CH_4$ (–) |
| 0 | $119 \times 10^{-8}$ | 159 | $60.6 \times 10^{-8}$ | 172 |
| 1.5 | $1.68 \times 10^{-8}$ | 0.92 | $0.80 \times 10^{-8}$ | 15 |
| | | | PDMS (7.5%) | |
| 0 | $118 \times 10^{-8}$ | 160 | $55.4 \times 10^{-8}$ | 185 |
| 1.5 | $1.71 \times 10^{-8}$ | 0.92 | $0.84 \times 10^{-8}$ | 30 |
| | | | PDMS (8.5%) | |
| 0 | $118 \times 10^{-8}$ | 160 | $39.4 \times 10^{-8}$ | 166 |
| 1.5 | $1.69 \times 10^{-8}$ | 0.93 | $0.81 \times 10^{-8}$ | 22 |

All silica DDR zeolite is also interesting for separating light gases and has been synthesized for the first time by Gies [194]. The first DDR zeolite membrane, prepared by Tomita *et al.* [195] on α-$Al_2O_3$ tube and by the one-step method, has exhibited a decrease in the permeance as a function of the gas kinetic diameters. In addition, the presence of water did not affect the permeation properties of the membrane due to its hydrophobic nature. Some years later, Himeno and coworkers have prepared a DDR membrane on tubular alumina support that showed better $CO_2$-$CH_4$ separation and carbon dioxide permeance. In mixed-gas permeation experiments, a $CO_2/CH_4$ selectivity of 200 and a $CO_2$ permeance of $3.0 \times 10^{-7}$ mol $m^{-2}s^{-1}Pa^{-1}$ ($T = 25\,°C$ and $P_{feed} = 2$ bar) have been measured [196]. The template used for the DDR synthesis is the 1-adamantane amine, and for its removal, very high temperatures (higher than 600 °C) are required. The membrane calcination caused defect formation for the high thermal stress developed. For this reason, it is essential to found a safe method for the activation of the membrane capable of preserving the gas permeation properties. In 2004, Heng *et al.* removed the template of silicalite membranes (with a thickness of 2 μm) at low temperature (200 °C) and in presence of a mixture of oxygen and ozone (50 g/$m^3$) [197]. Later, the same strategy was adopted by Gu and coworkers for the DDR zeolite membranes [198]. SEM analyses indicated the absence of cracks that usually are generated by carrying out the calcination in a traditional way. These membranes displayed $CO_2$ permeance of $3.5 \times 10^{-8}$ mol $m^{-2}$ $s^{-1}$ $Pa^{-1}$ and a very high separation factor (500) using an equimolar $CO_2$-$CH_4$ mixture as feed at 25 °C. Recently, DDR zeolite membranes have been synthesized with a conventional template (in reduced concentration), with inexpensive inorganic bases (NaOH, KOH, LiOH) as a mineralizing agent, and achieving the hydrothermal treatment in 3–6 h [199]. Very thin membranes and with interesting permeation properties have been prepared. Other results on the NG purification obtained by using small zeolite pore membranes are reported in Table 9.

In Fig. 12 is illustrated the separation factor versus the permeate flux for natural gas purification of different zeolite membranes (experimental tests have been performed in the same operating conditions: T = 20–25 °C; equimolar gas mixture).

The experimental results evidence as the better results in terms of separation factors are obtained with the small-pore zeolite membranes without aluminum in the zeolitic structure since the latter determines the defect formation in the zeolite film because it blocks the zeolitization and the formation of the layer. Fig. 12 also highlighted as at elevated separation factors correspond to low permeances and *viceversa*. The future challenge for the researchers will be based on the possibility of synthesizing very thin zeolite membranes with both elevated flux and separation factors, and high stability.

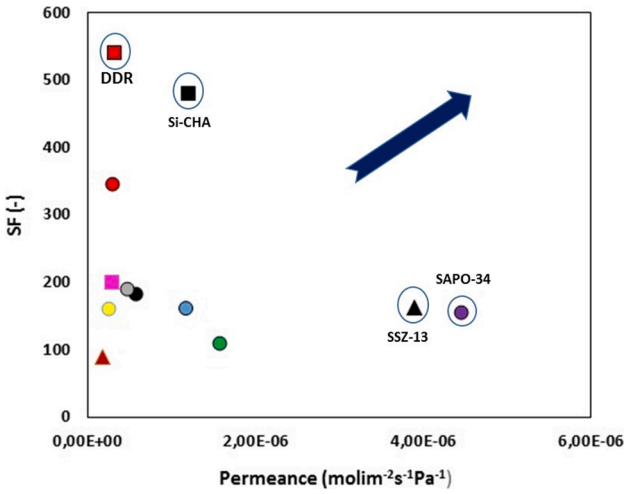


**Fig. 12.** $CO_2$-$CH_4$ separation factor versus $CO_2$ permeance for small pore zeolite membranes. Orange triangle: DDR zeolite membrane [75]; Blue circle: SApo-34 zeolite membrane [181,189]; Pink square: DDR zeolite membrane [196]; Black circle: SSZ-13 zeolite membrane [200]; Black triangle: SSZ-13 zeolite membrane [201]; Black square: Si-CHA zeolite membrane[202]; Red circle: SSZ-13 zeolite membrane [195,203]; Violet circle: SAPO-34 membrane [204]; Yellow circle: SAPO-34 membrane [81]; Green circle: SAPO-34 membrane [205]; Red square: DDR zeolite membrane [206]; Grey circle: DDR zeolite membrane [207]. Operating conditions: T = 20–25 °C; equimolar gas mixture. (For interpretation of the references to color in this figure legend, the reader is referred to the web version of this article.)

## 6. Zeolite membrane reactors

Process Intensification strategy is based on developing sustainable and cost-effective chemical process systems by reducing equipment size, energy consumption, and waste production [208]. A membrane reactor represents a process intensification technology where a chemical reaction and the separation step are combined in a single unit operation. This approach permits to obtain a higher conversion than the traditional process by using a compact and cost-effective reactor [209,210]. Membranes and reactors can be arranged in different configurations classified into three main groups: extractor, distributor, and contactor

**Table 9**
Small-pore zeolite membrane performance in $CO_2$-$CH_4$ separation.

| Zeolite-Type | Support | Operating conditions Gas test | $CO_2$ Permeance ($\times 10^{-7}$molm$^{-2}$s$^{-1}$Pa-$^{1}$) | $CO_2/CH_4$ (–) | Ref. |
|---|---|---|---|---|---|
| SSZ-13 | α-$Al_2O_3$ Tube | T = 30 °C, $P_{feed}$ = 2 bar equimolar gas mixture | 5.8 | 183 | [200] |
| SSZ-13 | α-$Al_2O_3$ Tube | T = 20 °C, $P_{feed}$ = 1.4 bar equimolar gas mixture | 39 | 162 | [201] |
| Si-CHA | α-$Al_2O_3$ Tube | T = 25 °C, $P_{feed}$ = 2 bar equimolar gas mixture | 12 | 480 | [202] |
| SSZ-13 | Mullite Tube | T = 25 °C, $P_{feed}$ = 2 bar equimolar gas mixture | 3.0 | 345 | [203] |
| SAPO-34 | α-$Al_2O_3$ Tube | T = 25 °C, $Pf_{eed}$ = 1.4 bar equimolar gas mixture | 44.6 | 155 | [204] |
| SAPO-34 | α-$Al_2O_3$ Tube | T = 25 °C, $Pf_{eed}$ = 2.0 bar equimolar gas mixture | 2.5 | 160 | [81] |
| SAPO-34 | α-$Al_2O_3$ Tube | T = 29 °C, $P_{feed}$ = 1.4 bar equimolar gas mixture | 15.7 | 109 | [205] |
| DDR | $SiO_2$ Disk | T = 30 °C, $P_{feed}$ = 1.0 bar equimolar gas mixture | 3.2 | 540 | [206] |
| DDR | α-$Al_2O_3$ Tube | T = 25 °C, $P_{feed}$ = 1.4 bar equimolar gas mixture | 4.7 | 190 | [207] |
| DDR | α-$Al_2O_3$ Disk | T = 24 °C, $P_{feed}$ = 2.0 bar 90% $CO_2$ –10% $CH_4$ | 1.8 | 90 | [75] |

[211,212]. When the membrane acts as an extractor, a reaction product is removed with an increase in the conversion (shifting the reaction equilibrium according to Le Chatelier's principle) [213]. As a distributor, the membrane controls the addition of a reactant(s) to reduce the side reactions [214]. In these two configurations, the membrane is catalytically inert and coupled with a traditional catalytic process. In the contactor, the membrane is catalytically active and ensures better interaction between reactants and active sites of the catalyst [215,216].

Today, 48% of hydrogen is produced by steam reforming (SR) of natural gas [215]. In the SR process, methane and steam produce hydrogen ($H_2$) and carbon monoxide (CO). Water-gas shift (WGS) reaction is used after the reforming process for increasing the hydrogen content. This reaction is exothermic and limited by thermodynamic equilibrium [217]; the use of an MR could improve the CO conversion by continuously removing a reaction product to overcome the chemical equilibrium limitation [218]. Kim et al. have demonstrated that a silicalite membrane improves the WGS process's performance [219]. The membrane has been prepared by the in *situ* method and modified by the on-stream catalytic cracking deposition (CCD) method. The CCD method allows controlling the silica deposition within a small part of the MFI channels near the membrane surface [220]. The experimental studies demonstrated as the conversion of the CO enhanced (98.5%) overcoming the equilibrium limit, operating as high temperature (>500 °C) and pressure (6 bar). Simulation studies have indicated as the zeolite MRs could achieve a very high CO conversion (≥99%) under these operating conditions: T > 500 °C, P = 30 atm, and $R_{H2O/CO}$ ~3.5 [220]. Arvanitis and coworkers obtained exciting results with an MFI zeolite membrane reactor [221,222]. The membrane was fabricated on α-$Al_2O_3$ tubular support by the one-step method and then modified using the CCD method [222]. The CO conversion, the hydrogen recovery, and the purity (in permeate product) obtained at different feed pressures are shown in Fig. 13.

The CO conversion with MR has exceeded the value obtained at the equilibrium. At each gas hourly space velocity (GHSV), the CO conversion increased with the feed pressure due to enhanced transport of hydrogen through the membrane (increased driving force). A conversion of 99.9% has been reached, performing the experiments at 15.7 bar and 7500 $h^{-1}$. The hydrogen removal increased with the feed pressure but at the same time decrease the purity of permeate ($y_{H2}$ = 78.2% at P = 15.7 bar; $y_{H2}$ = 65% at P = 19.5 bar) because the membrane exhibited a moderate $CO_2/H_2$ separation ($\alpha_{CO2/H2}$≈ 38). In Table 10 are reported other results obtained with zeolite membrane reactors in WGS process.

Dimethyl ether (DME) production has inspired increasing attention as an attractive route for large-scale $CO_2$ valorization [227]. DME is considered a sustainable alternative to diesel fuel for its high cetane number, low autoignition temperature, and low pollutant emission [228]. The reactions involved are:

Methanol synthesis : $CO + 2H_2 \leftrightarrow CH_3OH$

Methanol synthesis : $CO_2 + 3H_2 \leftrightarrow CH_3OH + H_2O$

Metanol dehydration : $2CH_3OH \leftrightarrow CH_3OCH_3 + H_2O$

Hydrocarbon formation (undesired) : $CO_2 + 3H_2 \leftrightarrow CH_4 + H_2O$

Water gas shift : $CO + H_2O \leftrightarrow CO_2 + H_2$

The removal of water from the reaction environment permits overcoming the thermodynamic limitation and avoiding the deactivation of the catalyst (blocking of the active sites). Iluta and coworkers have demonstrated by simulation study as the in situ $H_2O$ removal has improved the $CO_2$ conversion in methanol and DME productivity with a hydrophilic membrane in a fixed-bed reactor [229]. Fedosov and coworkers examined the dehydration of methanol to DME in a flow mode with a NaA zeolite membrane reactor (ZMR) and using γ-alumina as catalyst [230]. An improvement of the methanol conversion with the ZMR over the packed bed reactor has been found. A methanol conversion of 85% has been reached using the ZMR at 250 °C. In the traditional one, a conversion of only 61% has been achieved. Separation selectivity of the membrane and reactor design have been the limiting factors of the process. In 2016, Zhou et al. reported a novel bifunctional catalytic zeolite membrane reactor for methanol dehydration to DME [231]. The membrane reactor had a sandwich structure; one membrane (zeolite H-FAU) acted as the catalyst for the DME production. The other membrane (zeolite Na-LTA) worked as a separator for performing a selective removal of water. This novel membrane reactor permits high methanol conversion (90.9% at 310 °C) and a DME selectivity of about 100%. Recently, Rodriguez-Vega et al. studied the direct synthesis of DME employing a packed bed membrane reactor (PBMR) [228]. The catalytic tests have been carried out using a CuO-ZnO-$ZrO_2$/SAPO-11 as the catalyst (temperature range of 275–325 °C and pressure of 10–40 bar). The experimental results (illustrated in Fig. 14) have evidenced that the DME yield increased with the temperature (from 275 °C to 325 °C); methanol and paraffins yields also improved with a maximum of 3.7% and 1.1%, respectively. The conversion of $CO_2$ has been higher in the membrane reactor than the traditional one, in the temperature range evaluated. This result has been explained for the removal of water from the reaction medium. The DME selectivity also increased and remained almost constant at high temperatures (see Fig. 14b). Increasing the temperature also increased the selectivity of paraffins, that produced by methanation or Fischer-Tropsch reactions. The stability of the catalyst has lower in the temperature range 275 °C–300 °C (as shown in Fig. 14c)

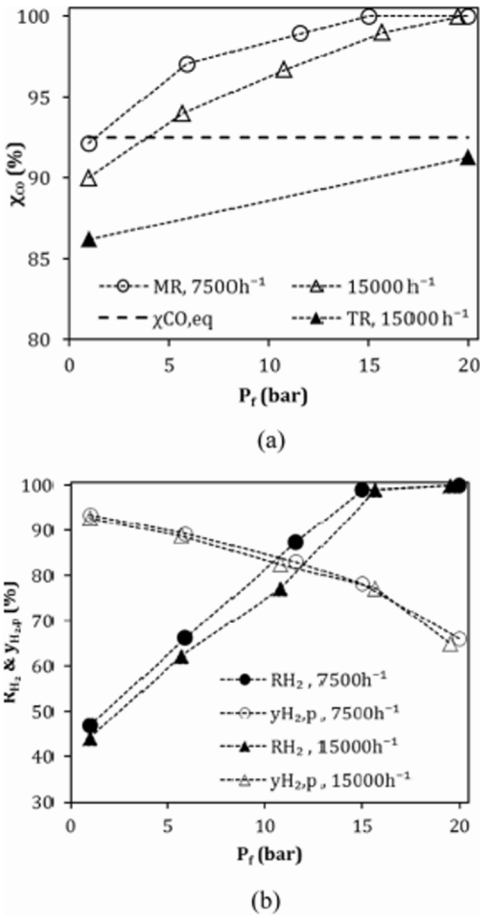


**Fig. 13.** Results of WGS reaction: (a) CO conversion ($\chi_{CO}$) (b) Hydrogen recovery ($R_{H2}$) and purity ($y_{H2,p}$) in permeate product as a function of the fed pressure ($P_f$) for MR and TR (T = 500 °C and $_{RH2O/CO}$ = 3.5); and [221]. Reproduced with permission of Elsevier. B.V. (2021).

**Table 10**
Zeolite membrane reactor performance in WGS process.

| Zeolite topology | Support | Temperature (°C) | Catalyst | CO conversion% | $H_2$ recovery (%) | References |
|---|---|---|---|---|---|---|
| MFI** | α-$Al_2O_3$-HF° | 350 | $Fe_2O_3/Cr_2O_3/Al_2O_3$ | 73.6 | 98.2 | [223] |
| MFI** | α-$Al_2O_3$-Disk | 300 | $Cu/Zn/Al_2O_3$ | 95.4 | – | [224] |
| MFI** | α-$Al_2O_3$-Tube | 550 | $Fe_{1.82}Ce_{0.18}O_3$ | 81.7 | 40 | [225] |
| MFI** | α-$Al_2O_3$-Disk | 550 | $Fe_{1.82}Ce_{0.18}O_3$ | >99 | >60 | [226] |

MFI = Mobil-Type Five; ** Membrane modified by catalytic cracking method; ° HF = Hollow fiber; °°α-$Al_2O_3$-Disk modified with yttria stabilized zirconia (YSZ) barrier layer to prevent the Al diffusion into the zeolite layer,

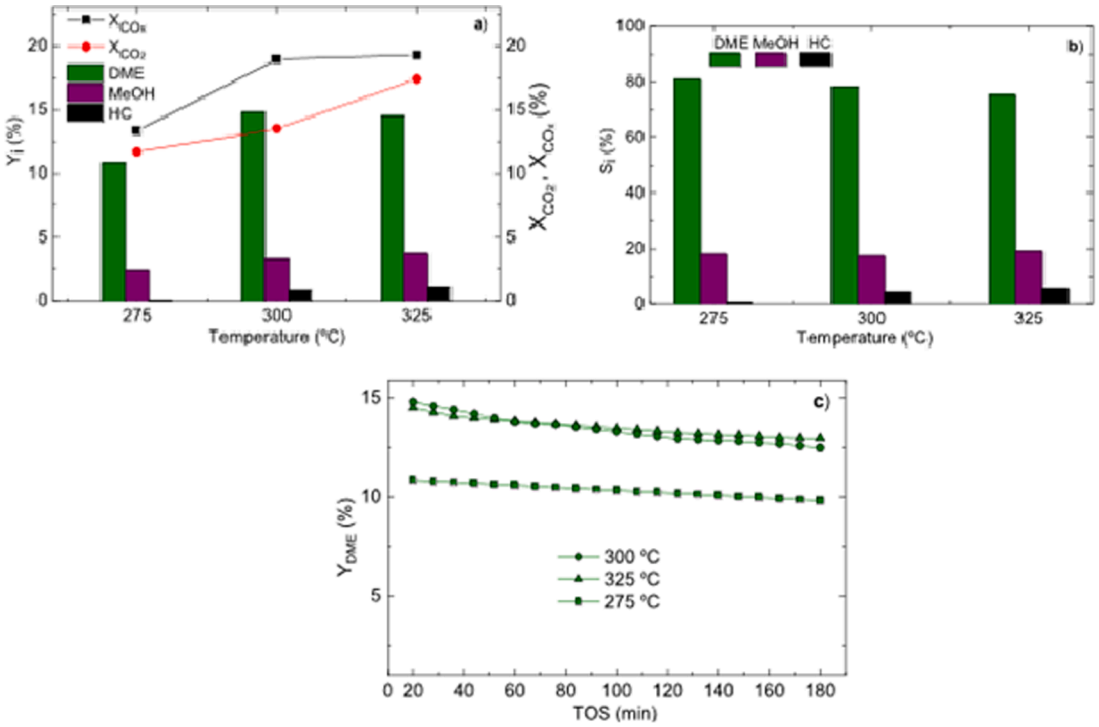


**Fig. 14.** Temperature effects on DME, MeOH, and hydrocarbons (HCs) yield and $CO_x$ and $CO_2$ conversion (a), on product selectivity (b) (at zero time on stream). DME yield with time on stream (c) at different reaction temperatures. (Reaction conditions: 30 bar; space–time of 10 $g_{cat}h^{-1}$ ($mol^{-1}$)) [228]. Reproduced with permission of Elsevier. B.V. (2021).

and higher at 325, probably due to catalyst sintering. DME and MeOH yield increased, and paraffin yield decreased by raising the pressure. In particular, increasing the pressure from 20 to 30 bar, the $CO_x$ conversion boosted from 8.8 to 17.9% and DME yield from 7.0 to 13.7%.

Zeolite membranes in MRs have also been applied as an extractor for performing other essential processes as the Fisher-Tropsch and the dehydrogenation of light alkanes to olefins.

The first process converts the syngas from natural gas or biomass into liquid hydrocarbons [232]. This promising clean technology is a potential alternative method to solve the shortage of liquid transport fuel [225,233]. In this process, the membrane removes a reaction product (water) to reduce the catalyst deactivation and increase the conversion [234]. The water can negatively affect the reaction rate due to the formation of $CO_2$ by the WGS reaction.

Catalytic dehydrogenation for alkene production seems to be an interesting alternative and environmentally friendly route for producing light olefins [235]. The demand for these chemical compounds is constantly growing because they are employed as building blocks in the industrial production of different solvents, chemicals, and polymers [236]. Today, the cracking of crude-oil-derived naphtha and fluid catalytic cracking of heavy oil are used for alkenes production [237]. These processes suffer from different limitations as high-energy demands, enormous $CO_2$ emissions, and low selectivity towards light olefins [237]. Dehydrogenation process is limited by thermodynamic equilibrium, and the hydrogen separation in a membrane reactor can help drive the reaction forward. The application of ZMRs in these processes is shown In Table 11.

A few papers on applying the zeolite membrane reactor as a distributor are present in the open literature. In 2001, Mota et al. used ZMR for the selective oxidation of n-butane to maleic anhydride [243]. This reaction is performed at an industrial scale, and most of the plants are conventional fixed-bed reactors [244]. The concentration of butane is very low (1.5%) due to the flammability of the $O_2/C_4$ mixture, which leads to very low productivity [244]. The researchers have used MFI zeolite membrane to distribute the oxygen and vanadium phosphate mixed oxide as catalyst. This configuration has permitted to low the concentration of oxygen by preventing dangerous concentration, and side reactions. The maleic anhydride productivity was three times higher than that observed with the conventional reactor.

Zeolite membranes are also used as catalytically active contactors and not necessarily permselective [211]. This configuration ensures a reduction of the catalyst particles aggregation, a better contact between reactants and catalyst active sites, and reduces by-passing and misdistribution present in a packed bed reactor. A zeolite membrane reactor as a contactor has been used for the CO selective oxidation (SelOx) for the carbon monoxide removal from $H_2$-rich gas streams produced by the reforming process [245,246]. This because the CO present in the hydrogen $H_2$ rich-streams poisons the anode of the proton exchange

**Table 11**
ZMR performance in Catalytic dehydrogenation of alkene.

| Zeolite topology | Support | Temperature (°C) | Catalyst | Reactant conversion% | Product selectivity (%) | References |
|---|---|---|---|---|---|---|
| ZSM-5 | -/Tubular | 310 | Iron* | CO (96) | – | [238] |
| SAPO-34 | -/Tubular | 600 | $Na_2O$-$Cr_2O_3$-$Al_2O_3$** | Propane (65–75) | Propylene (85) | [239] |
| MFI | α-$Al_2O_3$-Disk | 600 | Pt/$Al_2O_3$ | Ethane (22) | Ethylene (90%) | [240] |
| MFI | α-$Al_2O_3$-Disk | 600 | Pt/$Al_2O_3$ | Isobutane (27) | Isobutylene (97) | [241] |
| MFI | α-$Al_2O_3$-Disk | 600 | Pt/$Al_2O_3$ | Ethane (29) | Ethylene (97%) | [242] |

*Iron catalyst = 100Fe/5.26Cu/4.76 K/18.2SiO; ** $Na_2O$-$Cr_2O_3$-$Al_2O_3$ = 1% $Na_2O$-doped 20 %$Cr_2O_3$/80% $Al_2O_3$.

membrane fuel cells (PEM-FCs) used for electricity production [247].

In the SelOx process, a selective catalyst is required for avoiding hydrogen consumption since two competitive reactions occur:

$$2CO + O_2 \rightarrow 2CO_2$$

$$2H_2 + O_2 \rightarrow 2H_2O$$

Bernardo et al. have used NaY zeolite membranes loaded with Pt for CO SelOx [246]. The zeolite membranes characterized by different permeation properties have shown diverse catalytic performance. The effect of the feed pressure on the CO conversion obtained with catalytic zeolite membranes is illustrated in Fig. 15. A negligible impact of the pressure has been observed for the less permeable membranes (Q and H). A positive effect, on the contrary, has been found for the membranes more permeable (I and U). The authors have explained the effect of the pressure on the CO conversion considering two pathways in the membrane: zeolite pores and defects. When the CO permeates through the zeolite pores, the probability of interacting with the catalytic particles is very high due to the narrow space available. In this case, the pressure does not affect the CO conversion. When the CO passes through the defects (pores of the support), the contact between the reactant and the catalytic particles increases with the feed pressure.

CO SelOx experiments have been performed without the $CO_2$ in the feed stream, even if in a real SelOx process, the hydrogen rich gas stream from the WGS contains about 20–25% of $CO_2$. Recently, it has been demonstrated as the $CO_2$ in the feed stream has determined a lowering of the CO conversion by using the Pt/Na-Y zeolite membranes as catalytic systems [247]. This negative effect has been explained for the presence of the reverse water gas shift that limited the CO oxidation at high temperatures.

This section has shown the possibility of using zeolite membrane reactors in various processes to improve conversion, selectivity, or yield.

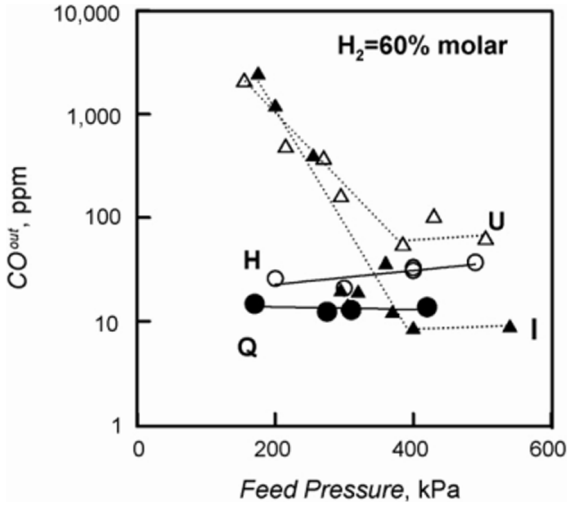


**Fig. 15.** CO concentration at the MR exit as a function of the pressure of the feed for various Pt/Na-Y membranes (Operating conditions: λ = 2; feed = 505 $cm^3$(STP)/min; T = 205 C) [246]. Reproduced with permission of Elsevier. B.V. (2021).

However, their wide application at an industrial scale could be possible by preparing highly selective, very thin, reproducible, and cost-effective membranes.

## 7. Future directions in the zeolite membrane field

In this section, the future research directions in the zeolite membrane field have been identified and discussed.

### 7.1. Application of zeolite membranes in solid state-batteries

Today, lithium ion batteries (LIBs) supply energy in different portable appliances as smartphones, notebooks, and also in electric vehicles [248], and their energy density reached the value of 260 Wh $kg^{-1}$ [249]. These devices are used as energy storage for converting chemical energy into electrical energy and *vicecersa*. Lithium-air batteries (called too lithium-oxygen batteries) are a good candidate as a new generation of energy storage systems due to their high theoretical energy density (~900 Wh $kg^{-1}$) [250]. In these batteries, lithium oxidation (at the anode) and the oxygen reduction (obtained from the air) at the cathode happen [251,252]. Unfortunately, the corrosion of the lithium anode, the decomposition and volatilization of the electrolyte, and the production of harmful by-products on the cathode still need to be solved [252]. In recent years, intense research activity was devoted to the solid-state lithium-air batteries (SSLABs) that are safer and with improved electrochemical and thermal stability and better energy/power density [253,254]. Inorganic solid electrolytes (e.g., $Li_7La_3Zr_2O_{12}$(LLZO), perovskite $Li_{3.3}La0._{56}TiO_3$ (LLTO), and superionic sodium conductor) exhibit high conductivity and stability [255]. However, they cannot be used in solid-state Li-air batteries being unstable towards lithium metal and air and for the difficulty of constructing low-resistance interfaces [256]. In this year, Chi et al. have used NaX zeolite membrane exchanged with the lithium ions as a solid state electrolyte for the SSLABs due to its low conductivity, elevated ion conductivity, and good stability toward the different battery components [257]. The zeolite membrane has been prepared on the stainless-steel substrate with a secondary growth method and dip-coating as a seeding procedure [258], and the LiX zeolite membrane through the cationic exchange has been prepared. Li-ions are used as the counter-ions of LiX zeolite, and so the $Li^+$, formed at the anode, can migrate freely across the membrane. This new battery exhibits good performance in terms of safety, flexibility, and long cycle life in the presence of air.

Another good alternative to the LIBs is the lithium-sulfur (Li-S) batteries for their low cost, non-toxicity, and very high specific energy density (~2500Whkg$^{-1}$) [259,260]. During the charge and discharge process, in Li-S cells at the cathode, a complex reaction occurs that involves the formation of lithium polysulphides ($Li_2S_x$, $1 < x < 8$) [261]. Their commercialization is blocked by the shuttle effect of the polysulphides [253,261]. During the shuttle effect, polysulfides diffuse into the surface of the lithium anode, whereas lithium polysulfide are produced with a short segment length ($Li_2S$ and/or $Li_2S_2$) [262]. Then, the short-chain lithium polysulfides diffuse back to the cathode with the formation of long-chain lithium polysulfides [262]. As a result, there is a continuous loss of active material from the electrode, low coulombic-efficiency, and short battery life [263]. Recently, Wang et al.

demonstrated the possibility to suppress the shuttle effect by using a zeolite membrane as a separator in the battery [264]. A thin NaX layer has been grown on the Celgard separator (used as a support). The LiNaX-celgard membrane has been prepared by cationic exchange. The separator-zeolite membrane-based possesses different benefits as good Li-ion conductivity and the possibility to inhibit the shuttle effect due to a strong electrostatic repulsive force between the negative charges of the zeolite membrane and those of lithium polysulfides (PSs) [264]. In addition, being the zeolite pore size smaller than the molecular dimension of the PSs a molecular sieving mechanism is also exerted. In Fig. 16 is illustrated the capacity of LiX/Celgard separator to depress the shuttle of sulfur employing as molecule probe the $Li_2S_6$ in a H-type electrolytic cell during the experiment.

The solid-state batteries zeolite membrane-based for their superior flexibility, safety, and stability open a new route to develop rechargeable battery and other energy storage devices characterized by high-performance and shorten the time needed to bring them on the market.

### 7.2. Potential application of zeolite membranes in the Space engineering

In the last years, the funding for Space exploration has undergone a substantial increase for correlated researches [265]. For example, in collaboration with the Russian space agency, the European Space Agency (ESA) organized the ExoMars program that comprises missions for searching signs of past life on Mars [266]. An International Lunar Research Station has also been planned between Russia and China [267]. In the beginning, a robotic lunar mission will be organized and the building of the lunar station. Finally, different human-crewed missions will be planned for finding natural resources on the lunar soil and new systems for electricity production. Long missions in Space require oxygen and freshwater, solid and liquid waste management, and atmosphere revitalization [268]. Membrane technology can offer exciting solutions for overcoming these challenges. Recently, the European Space Agency has presented the possibility of recovering water and air aboard the International Space Station (ISS), and the scheme is shown in Fig. 17 [269].

Initially, the alkaline fuel cells (AFCs) have been used by NASA in the Space program for producing electricity and water for spacecraft crew [269,270]. The First application of fuel cells in the aerospace sector dates back to 1960 (General Electric developed the first Proton Exchange Membrane fuel cell (PEMFC) for Gemini missions (NASA)). [271]. Today, the NASA Glenn Research Center, the section of NASA about the research on the technology of fuel cells, focused the attention on other PEMFCs that use hydrogen as fuel and the water is a reaction product [272]. PEMFCs seem to be appropriate for the Space mission being are very compact and capable of producing high power densities. However, the water produced prevents the reactants from accessing the catalyst's active sites with a significant fuel cell performance reduction [273]. In addition, the bipolar plates are a substantial part of the PEM fuel cell stack and contribute to 80% of the fuel cell's weight, 50% of its volume, and 40% of its cost [274]. It is essential to find materials inexpensive, lighter with high mechanical strength, high electrical and thermal conductivity [275] to develop new PEM-FCs for aerospace applications.

Air dehumidification in a spacecraft is performed with a condensing heat exchanger (CHX) [276], where the hydrophilic coating (on the surface of CHX) absorbs the condensate water, and a mechanical rotary separator is used for the air–water mixture separation [277]. However, one of the biggest problems is that, in microgravity conditions, the air–water separation is difficult to perform [278]. After prolonged use, the hygroscopic coating may dissolve and carried away by the air-flow by the separator, and the separator will occlude [279]. These problems could be overcome using hydrophilic zeolite membranes made in sheet form [280,281]

The scheme reported in Fig. 17 also indicates the possibility to produced methane with a Sabatier reactor and by using as reactants hydrogen (produced *via* electrolysis of water) and $CO_2$ (captured by the atmosphere) [282]. In this process, hydrophilic zeolite membranes could be used for the water removal by enabling a significant improvement of the $CO_2$ conversion compared to the traditional reactor performance [283-286].

Materials utilized in Space missions are exposed to very hostile environmental conditions in which products used on earth should function. Even if this does not happen, in fact, polymeric materials are susceptible to the action of solar and cosmic radiations by manifesting peel-off, color changes, and cracking [287]. The NASA Goddard Space Flight Center has developed a sprayable zeolite coating. The coatings are capable "to capture" molecular species near sensitive surfaces and lower the risks associated with material outgassing in vacuum environments for aerospace applications [288,289].

Considering all the aspects analyzed in this section, zeolite membranes withstanding at high temperatures for a long time and in aggressive environment for their high chemical stability can solve different problems present in the Space engineering sector.

## 8. Conclusions and perspectives

Zeolite membranes can separate gas or liquid mixtures with high separation factors due to their pore size at the molecular scale and adsorption property. In addition, they present high thermal and chemical resistance and so can be utilized when polymer membranes do not operate.

During the years, thanks to intensive research activities, various problems were solved. First of all, a synthesis method (secondary growth) was identified as more reproducible and could prepare thin zeolite layers. However, very high-quality membranes require the

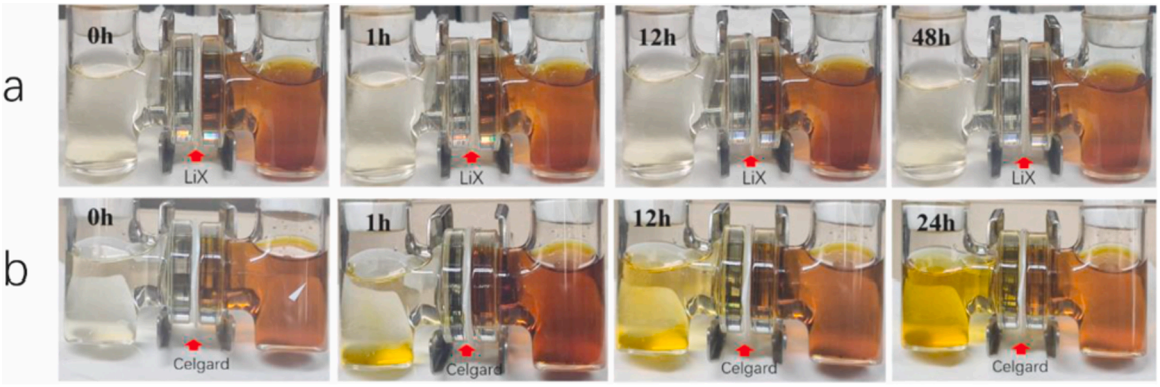


**Fig. 16.** Pictures of $Li_2S_6$ diffusion through the LiX/Celgard (a) and pristine Celgard (b) separators sandwiched between two branch tubes of H-type electrolytic cells [264]. Reproduced with permission of Elsevier. B.V. (2021).

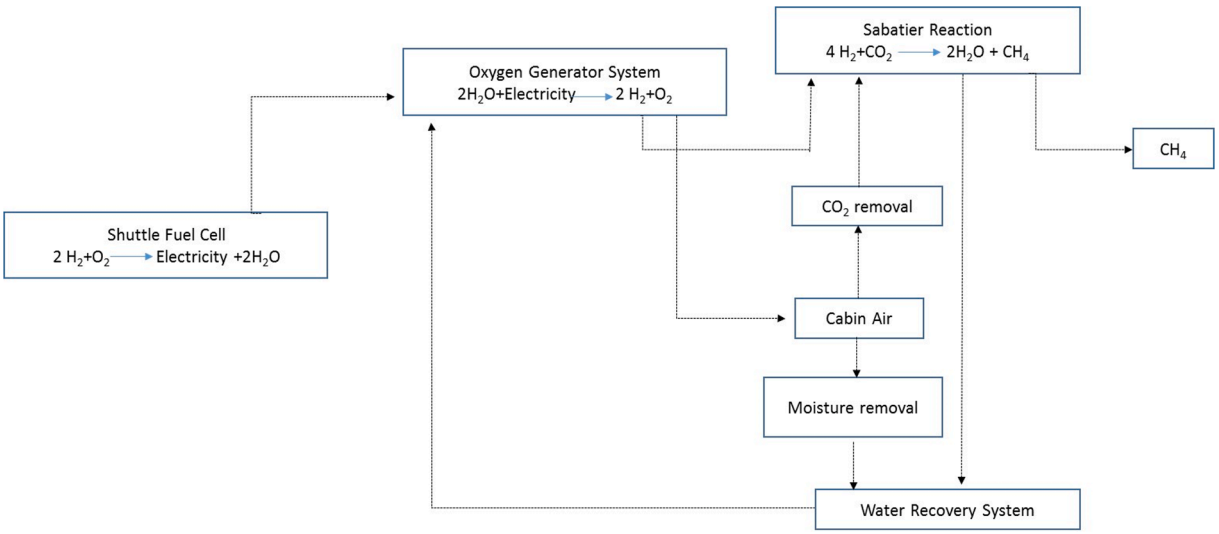


**Fig. 17.** Scheme about the supply of oxygen, water, and fuel in Space. [Adapted from 269].

absence of defects or pinholes in the zeolitic layer because the permeation through the defects determines a selectivity reduction. Different routes have been followed for improving the membrane performance. Innovative calcination procedures and curing treatments have been also developed to enhance the permeation property of these membranes. Anyway, despite all these efforts, many problems remain. Very thin (<100 nm) membranes defect-free (without grain boundary, crack, and pinhole) and with both high permeance and selectivity represent the biggest challenges in this field. Another drawback is the high membrane cost that could be overcome by using cheaper supports and reducing as much as possible the membrane thickness to obtain high flux per unit area. Indeed, considering all these aspects, applying these membranes on a large scale is limited to a few zeolite types for various organic solvent dehydration utilizing the pervaporation process. Besides, these commercial membranes used in gas separation processes exhibit low separation factors. In the pervaporation, the defects are plugged by the water molecules for capillarity. While, during the gas separations, the defects participate in the separation process.

These membranes also showed attractive performance in the desalination process, and the results present in the open literature were intensely discussed.

Zeolite membranes characterized by small pore size (as SSZ-13, SAPO-34, DD3R) attracted more attention in the scientific community for high efficiency in small-gas separations in a wide temperature and pressure range. High silica membranes for their hydrophobic nature and remarkable chemical resistance would be necessary for the presence of water in the gaseous mixtures and aggressive environments. ZMRs application in various catalytic processes has also been reported and discussed.

The future direction of the research in this field has also been presented.

## Declaration of Competing Interest

The authors declare that they have no known competing financial interests or personal relationships that could have appeared to influence the work reported in this paper.

## References

[1] E. Drioli, A.I. Stankiewicz, F. Macedonio, Membrane engineering in process intensification-An overview, J. Membr. Sci. 380 (2011) 1–8.
[2] F. Macedonio, E. Drioli, A.A. Gusev, A. Bardow, R. Semiat, M. Kurihara, Efficient technologies for worldwide clean water supply, Chem. Eng. Process. Process Intensif. 51 (2012) 2–17.
[3] N. MacDowell, N. Florin, A. Buchard, J. Hallett, A. Galindo, G. Jackson, et al., An overview of CO capture technologies, Ener. Env. Sci. 3 (2010) 1645–1669.
[4] P.S. Goh, A.F. Ismail, A review on inorganic membranes for desalination and wastewater T treatment, Desalination 434 (2018) 60–80.
[5] Y. Xia, M. Zhang, D.C.W. Tsang, N. Geng, D. Lu, L. Zhu, A.D. Igalavithana, P. D. Dissanayake, J. Rinklebe, X. Yang, Y.S. Ok, Recent advances in control technologies for non-point source pollution with nitrogen and phosphorous from agricultural runoff: current practices and future prospects, Appl. Biol. Chem. 63 (2020) 1–13.
[6] A. Alkaisi, R. Mossad, A. Sharifian-Barforoush, A review of the water desalination systems integrated with renewable energy, Energy Procedia 110 (2017) 268–274.
[7] P. Bai, M.Y. Jeon, L. Ren, C. Knight, M.W. Deem, M. Tsapatsis, J.I. Siepmann, Discovery of optimal zeolites for challenging separations and chemical transformations using predictive materials modeling, Nat. Commun. 6 (2015) 1–9.
[8] H.N. Tran, P.V. Viet, H. Chao, Surfactant modified zeolite as amphiphilic and dual-electronic adsorbent for removal of cationic and oxyanionic metal ions and organic compounds, Ecotoxicol. Environ. Saf. 147 (2018) 55–63.
[9] P. Frontera, S. Candamano, A. Macario, F. Crea, L.A. Scarpino, P.L. Antonucci, Ferrierite zeolitic thin-layer on cordierite honeycomb support by clear solutions, Mater. Lett. 104 (2013) 72–75.
[10] H. Zhang, W. Zhang, C. Shuang, Combination of Na-modified zeolite and anion exchange resin for advanced treatment of a high ammonia-nitrogen content municipal effluent, J. Colloid. Interface Sci. 468 (2016) 128–135.
[11] A. Ates, G. Akgül, Modification of natural zeolite with NaOH for removal of manganese in drinking water, Powder Technol. 287 (2016) 285–291.
[12] S. Boycheva, D. Zgureva, H. Lazarovac, M. Popova, Comparative studies of carbon capture onto coal fly ash zeolites Na-X and Na-Ca-X, Chemosphere 271 (2021) 129505-.
[13] A.A. Ahmed, Z.H. Yamani, Synthesis and characterization of $SnO_2$-modified ZSM-5 zeolite for hydrogen gas sensing, Mater. Chem. Phys. 259 (2021), 124181.
[14] J. Caro, M. Noack, Zeolite membranes-recent developments and progress, Micropor. Mesopor. Mater. 115 (2008) 215–233.
[15] C. Zhang, L. Peng, J. Jiang, X. Gu, Mass transfer model, preparation and applications of zeolite membranes for pervaporation dehydration: A review, Chin. J. Chem. Eng. 25 (2017) 1627–1638.
[16] P. Peng, X. Gao, Z.F. Yan, S. Mintova, Diffusion and catalyst efficiency in hierarchical zeolite catalysts, Natl. Sci. Rev. 11 (2020) 1726–1742.
[17] J. Ma, J. Shao, Z. Wang, Y. Yan, Preparation of zeolite NaA membranes on macroporous alumina supports by secondary growth of gel layers, Ind. Eng. Chem. Res. 65 (2014) 6121–6130.
[18] J. Jiang, X. Wang, Y. Zhang, D. Liu, X. Gu, Fabrication of pure-phase CHA zeolite membranes with ball-milled seeds at low K+ concentration, Micropor. Mesopor. Mater. 215 (2015) 98–108.
[19] R. Bedard, C. Liu, Recent Advances in Zeolitic Membranes, Annu. Rev. Mater. Res. 48 (2018) 83–110.
[20] E.R. Geus, M.J. denExter, H. vanBekkum, Synthesis and characterization of zeolite (MFI) membranes on porous ceramic supports, J. Chem. Soc, Faraday Trans. 88 (1992) 3101–3109.
[21] C. Feng, K.C. Khulbe, T. Matsuura, R. Farnood, A.F. Ismail, Recent progress in zeolite/zeotype membranes, J. Membr. Sci. Res. 1 (2015) 49–72.
[22] M.C. Lovallo, A. Gouzinis, M. Tsapatsis, Synthesis and characterization of oriented MFI membranes prepared by secondary growth, AICHE J. 44 (1998) 1903–1913.
[23] M.C. Lovallo, M. Tsapatsis, Preferentially oriented submicron silicalite membranes, AICHE J. 42 (1996) 3020–3029.

[24] K. Sato, T. Nakane, High reproducible fabrication method for industrial production of high flux NaA zeolite membrane, J. Membr. Sci. 301 (2007) 151–161.
[25] K. Kusakabe, T. Kuroda, S. Mooroka, Separation of carbon dioxide from nitrogen using ion-exchanged faujasite-type zeolite membranes formed on porous support tubes, J. Membr. Sci. 148 (1998) 13–23.
[26] Y. Hasegawa, K.I. Sotowa, K. Kusakabe, S. Morooka, The influence of feed composition on CO oxidation using zeolite membranes loaded with metal catalysts, Micropor. Mesopor. Mater. 53 (2002) 37–43.
[27] Y.S. Chun, K. Ha, Y.J. Lee, J.S. Lee, H.S. Kim, et al., Diisocyanates as novel molecular binders for monolayer assembly of zeolite crystals on glass, Chem. Commun. 65 (2002) 1846–1847.
[28] A. Huang, F. Liang, F. Steinbach, J. Caro, Preparation and separation properties of LTA membranes by using 3-aminopropyltriethoxysilane as covalent linker, J. Membr. Sci. 350 (2010) 5–9.
[29] Y. Yan, T. Bein, Zeolite thin films with tunable molecular sieve function, J. Am. Chem. Soc. 117 (1995) 9990–9994.
[30] T. Yan, Bein, Molecular recognition on acoustic wave devices: sorption in chemically anchored zeolite monolayers, J. Phys. Chem. 96 (1992) 9387–9393.
[31] K. Ha, Y.J. Lee, H.J. Lee, K.B. Yoon, Facile assembly of zeolite monolayers on glass, silica, alumina, and other zeolites using 3-halopropylsilyl reagents as covalent linkers, Adv. Mater. 12 (2000) 1114–1117.
[32] A. Kulak, Y. Lee, Y.S. Park, K.B. Yoon, Orientation-controlled monolayer assembly of zeolite crystals on glass and mica by covalent linkage of surface-bound epoxide and amine groups, Angew. Chem. Int. Ed. 39 (2000) 950–953.
[33] M. Pera-Titus, J. Llorens, F. Cunill, R. Mallada, J. Santamarıa, Preparation of zeolite NaA membranes on the inner side of tubular supports by means of a controlled seeding technique, Catal. Today 104 (2005) 281–287.
[34] A. Garofalo, L. Donato, E. Drioli, A. Criscuoli, M.C. Carnevale, O. Alharbi, S. A. Aljlil, C. Algieri, Supported MFI zeolite membranes by cross flow filtration for water treatment, Sep. Purif. Technol. 137 (2014) 28–35.
[35] A. Garofalo, M.C. Carnevale, L. Donato, E. Drioli, O. Alharbi, S.A. Aljlil, A. Criscuoli, C. Algieri, Scale-up of MFI zeolite membranes for desalination by vacuum membrane distillation, Desalination 397 (2016) 205–212.
[36] A. Xomeritakis, A. Gouzinis, S. Nair, T. Okubo, M. He, R.M. Overney, M. Tsapatsis, Growth, microstructure, and permeation properties of supported zeolite (MFI) films and membranes prepared by secondary growth, Chem. Eng. Sci. 54 (1999) 3521–3531.
[37] X. Wang, Z. Yang, C. Yu, L. Yin, C. Zhang, X. Gu, Preparation of T-type zeolite membranes using a dip-coating seedingsuspension containing colloidal $SiO_2$, Micropor. Mesopor. Mater. 197 (2014) 17–25.
[38] M. Lassinantti, J. Hedlund, J. Sterte, Faujasite-type films synthesized by seeding, Micropor. Mesopor. Mat. 38 (2000) 25–34.
[39] C. Algieri, P. Bernardo, G. Barbieri, E. Drioli, A novel seeding procedure for preparing tubular NaY zeolite membranes, Micropor. Mesopor. Mater. 119 (2009) 129–136.
[40] A. Huang, Y.S. Lin, W. Yang, Synthesis and properties of A-type zeolite membranes by secondary growth method with vacuum seeding, J. Membr. Sci. 245 (2004) 41–51.
[41] Z. Wang, Q. Ge, J. Gao, J. Shao, C. Liu, Y. Yan, High-performance zeolite membranes on inexpensive large-pore supports: highly reproducible synthesis using a seed paste, ChemSus. Chem 4 (2011) 1570–1573.
[42] X. Chen, J. Wang, D. Yin, J. Yang, J. Lu, Y. Zhang, Z. Chen, High-performance zeolite T membrane for dehydration of organics by a new varying temperature hot-dip coating method, AIChE J. 59 (2013) 936–947.
[43] H. Li, J. Wang, J. Xu, X. Meng, B. Xu, J. Yang, S. Li, J. Lu, Y. Zhang, X. He, D. Yin, Synthesis of zeolite NaA membranes with high performance and high reproducibility on coarse macroporous supports, J. Membr. Sci. 444 (2013) 513–522.
[44] T.C.T. Pham, T.H. Nguyen, K.B. Yoon, Gel free secondary growth of uniformly oriented Silica MFI zeolite films and application for xylene separation, Angew. Chem. Int. Ed. 52 (2013) 8693–8698.
[45] W. Chaikittisilp, M.E. Davis, T. Okubo, $TPA^+$ mediated conversion of silicon wafer into preferentially-oriented MFI zeolite film under steaming, Chem. Mater. 19 (2007) 4120–4122.
[46] K. Ueno, H. Negishi, T. Okuno, H. Tawarayama, S. Ishikawa, M. Miyamoto, S. Uemiya, Y. Oumi, Effects of seed crystal type on the growth and microstructures of silicalite-1 membranes on tubular silica supports via gel-free steam-assisted conversion, Micropor. Mesopor. Mat. 289 (2019), 109645.
[47] H. Negishi, S. Reuß, W. Schwieger, A.R. Boccaccini, Preparation of ZSM-5 zeolite membranes by combined hydrothermal synthesis and electrophoretic deposition, Key Eng. Mater. 654 (2015) 47–52.
[48] Y. Li, W. Yang, Microwave synthesis of zeolite membranes: A review, J. Membr. Sci. 316 (2008) 3–17.
[49] Y. Li, H. Chen, J. Liu, W. Yang, Microwave synthesis of LTA zeolite membranes without seeding, J. Membr. Sci. 277 (2006) 230–239.
[50] L.W. Shin, T.C. Thian, S. Bhatia, Synthesis, characterization and pervaporation properties of microwave synthesized zeolite A membrane, Desalination 277 (2011) 383–389.
[51] L. Wang, J. Yang, J. Wang, W. Raza, G. Liu, J. Lu, Y. Zhang, Microwave synthesis of NaA zeolite membranes on coarse macroporous α-$Al_2O_3$ tubes for desalination, Micropor. Mesopor. Mat. 306 (2020), 110360.
[52] T.L. Chew, A.L. Ahmad, S. Bhatia, Ba-SAPO-34 membrane synthesized from microwave heating and its performance for CO2/CH4 gas separation, Chem. Eng. J. 171 (2011) 1053–1059.
[53] N.E. Gordina, R.N. Rumyantsev, T.N. Borisova, A.E. Kolobkova, E.V. Tsvetova, E. E. Afanas'eva, E.S. Severgina, V.Y. Prokof'ev, Use of combinations of ultrasonic treatment and microwave crystallization to intensify the synthesis of LTA zeolite membranes, Pet. Chem. 61 (2021) 292–298.
[54] L. Li, J. Li, L. Cheng, J. Wang, J. Yang, Microwave synthesis of high-quality mordenite membrane by a two-stage varying heating-rate procedure, J. Membr. Sci. 612 (2020), 118479.
[55] K. Sun, B. Liu, S. Zhong, A. Wu, B. Wang, R. Zhou, H. Kita, Fast preparation of oriented silicalite-1 membranes by microwave heating for butane isomer separation, Sep. Purif. Technol. 219 (2019) 90–99.
[56] M. Wang, M. Lu Bai, L. Li, M. Gao, P. Wang, Y. Zhang Rao, Ultrafast synthesis of thin all-silica DDR zeolite membranes by microwave heating, J. Membr. Sci. 572 (2019) 567–579.
[57] J. Gascon, F. Kapteijn, B. Zornoza, V. Sebastián, C. Casado, J. Coronas, Practical approach to zeolitic membranes and coatings: state of the art, opportunities, barriers, and future perspectives, Chem. Mater. 24 (2012) 2829–2844.
[58] Z. Liu, T. Wakihara, K. Oshima, K.D. Nishioka, Y. Hotta, S.P. Elangovan, Y. Yanaba, T. Yoshikawa, W. Chaikittisilp, T. Matsuo, T. Takewaki, T. Okubo, Widening synthesis bottlenecks: realization of ultrafast and continuous-flow synthesis of high-silica zeolite SSZ-13 for $NO_x$ removal, Angew. Chem. 54 (2015) 5683–5687.
[59] Z. Liu, T. Wakihara, D. Nishioka, K. Oshima, T. Takewaki, T. Okubo, One-minute synthesis of crystalline microporous aluminophosphate ($AlPO_4$-5) by combining fast heating with a seed-assisted method, Chem. Commun. 50 (2014) 2526–2528.
[60] Z. Liu, T. Wakihara, C. Anand, S.H. Keoh, D. Nishioka, Y. Hotta, T. Matsuo, T. Takewaki, T. Okubo, Ultrafast synthesis of silicalite-1 using a tubular reactor with a feature of rapid heating, Micropor. Mesopor. Mater. 223 (2016) 140–144.
[61] L. Bai, N. Chang, M. Li, Y. Wang, G. Nan, Y. Zhang, D. Hu, G. Zeng, W. We, Ultrafast synthesis of thin SAPO-34 zeolite membrane by oil-bath heating, Micropor. Mesopor. Mater. 241 (2017) 392–399.
[62] H. Tang, L. Bai, M. Wang, Y. Zhang, M. Li, M. Wang, L. Kong, N. Xu, Y. Zhang, P. Rao, Fast synthesis of thin high silica SSZ-13 zeolite membrane using oil-bath heating, Int. J. Hydrog. Energy 44 (2019) 23107–23119.
[63] Z.P. Lai, G. Bonilla, I. Diaz, J.G. Nery, K. Sujaoti, M.A. Amat, E. Kokkoli, O. Terasaki, R.W. Thompson, M. Tsapatsis, D.G. Vlachos, Microstructural optimization of a zeolite membrane for organic vapor separation, Science 300 (2003) 456–460.
[64] T.C.T. Pham, H.S. Kim, K.B. Yoon, Growth of uniformly oriented silica MFI and BEA zeolite films on substrates, Science 3342 (2011) 1533–1538.
[65] M. Zhou, D. Korelskiy, P.C. Ye, M. Grahn, J. Hedlund, A Uniformly Oriented MFI Membrane for Improved $CO_2$ Separation, Angew. Chem. Int. Ed. 53 (2014) 3492–3495.
[66] Y. Peng, X.F. Lu, Z.B. Wang, Y.S. Yan, Fabrication of b-Oriented MFI Zeolite Films under Neutral Conditions without the Use of Hydrogen Fluoride, Angew. Chem., Int. Ed. 54 (2015) 5709–5712.
[67] A. Wu, C. Tang, S. Zhong, B. Wang, J. Zhou, R. Zhou, Synthesis optimization of (h0h)-oriented silicalite-1 membranes for butane isomer separation, Sep. Purif. Tech. 214 (2019) 51–60.
[68] K. Varoon, X. Zhang, B. Elyassi, D.D. Brewer, M. Gettel, S. Kumar, J.A. Lee, S. Maheshwari, A. Mittal, C.Y. Sung, M. Cococcioni, L.F. Francis, A.V. McCormick, K.A. Mkhoyan, M. Tsapatsis, Dispersible exfoliated zeolite nanosheets and their application as a selective membrane, Science 334 (2011) 72–75.
[69] Z. Cao, S. Zeng, Z. Xu, A. Arvanitis, S. Yang, X. Gu, J. Dong, Ultrathin ZSM-5 zeolite nanosheet laminated membrane for high-flux desalination of concentrated brines, Sci. Adv. 4 (2018) 1–10.
[70] B. Min, S. Yang, A. Korde, Y.H. Kwon, C.W. Jones, S. Nair, Continuous Zeolite MFI Membranes Fabricated from 2D MFI nanosheets on Ceramic Hollow Fibers, Angew. Chem. Int. Ed. 58 (2019) 8201–8205.
[71] B. Liu, H. Kita, K. Yogo, Preparation of Si-rich LTA zeolite membrane using organic template-free solution for methanol dehydration, Sep. purif. Tec. 230 (2020), 116533.
[72] J. Choi, H.K. Jeong, M.A. Snyder, J.A. Stoeger, R.I. Masel, M. Tsapatsis, Grain boundary defect elimination in a zeolite membrane by rapid thermal processing, Science 31 (2009) 590–593.
[73] N. Chang, H. Tang, L. Bai, Y. Zhang, G. Zeng, Optimized rapid thermal processing for the template removal of SAPO-34 zeolite membranes, J. Membr. Sci. 552 (2018) 13–21.
[74] S. Yan, H. Maeda, K. Kusakabe, S. Morooka, Y. Akiyama, Hydrogen-permselective $SiO_2$ membrane formed in pores of alumina support tube by chemical vapor deposition with tetraethylorthosilicate, Ind. Eng. Chem. Res. 33 (1994) 2096–2101.
[75] S. Yang, Z. Cao, A. Arvanitis, X. Sun, Z. Xu, J. Dong, DDR-type zeolite membrane synthesis, modification and gas permeation studies, J. Membr. Sci. 505 (2016) 194–204.
[76] A. Simona, H. Richter, B. Reif, M. Schuelein, D. Sanwald, W. Schwieger, Evaluation of a method for micro-defect sealing in ZSM-5 zeolite membranes by chemical vapor deposition of carbon, Sep. Purif. Technol. 219 (2019) 180–185.
[77] H. Maghsoudi, Defects of zeolite membranes: Characterization, modification and post-treatment techniques, Sep. Purif. Rev. 45 (2016) 169–192.
[78] Y. Yan, M.E. Davis, G.R. Gavalas, Preparation of highly selective zeolite ZSM-5 membranes by a post-synthetic coking treatment, J. Membr. Sci. 123 (1997) 95–103.
[79] Y. Hirota, K. Watanabe, Y. Uchida, Y. Egashira, K. Yoshida, Y. Sasaki, N. Nishiyama, Coke deposition in the SAPO-34 membranes for examining the effects of zeolitic and non-zeolitic pathways on the permeation and separation

properties in gas and vapor permeations, J. Membr. Sci. 415–416 (2012) 176–180.
[80] W. Chiu, I.S. Park, K. Shqau, J. White, M. Schillo, W. Ho, P. Dutta, H. Verweij, Post-synthesis defect abatement of inorganic membranes for gas separation, J. Membr. Sci. 377 (2011) 182–190.
[81] Y. Mu, H. Chen, H. Xiang, L. Lan, Y. Shao, X. Fan, C. Hardacre, Defects-healing of SAPO-34 membrane by post-synthesis modification using organosilica for selective $CO_2$ separation, J. Membr. Sci. 575 (2019) 80–88.
[82] R. Zhou, H. Wang, B. Wang, X. Chen, S. Li, M. Yu, Defect-patching of zeolite membranes by surface modification using siloxane polymers for $CO_2$ separation, Ind. Eng. Chem. Res. 54 (2015) 7516–7523.
[83] H. Chaudhari, Y.S. Kwon, M.Y. Shon, S.E. Nam, Y.I. Park, Stability and pervaporation characteristics of PVA and its blend with PVAm membranes in a ternary feed mixture containing highly reactive epichlorohydrin, RSC Adv. 9 (2019) 5908–5917.
[84] R. Castro-Munoz, M.Z. Ahmad, V. Fíla, Tuning of nano-based materials for embedding into low-permeability polyimides for a featured gas separation, Front. Chem. 7 (2020) 1–14.
[85] R.W. Baker, J.G. Wijmans, Y. Huang, Permeability, permeance and selectivity: a preferred way of reporting pervaporation performance data, J. Membr. Sci. 348 (2010) 346–352.
[86] Y. Song, F. Pan, Y. Li, K. Quan, Z. Jiang, Mass transport mechanisms within pervaporation membrane, Front. Chem. Sci. Eng. 13 (2019) 458–474.
[87] M.C. Burshe, S.B. Sawant, J.B. Joshi, V.G. Pangarkar, Sorption and permeation of binary water-alcohol systems through PVA membranes crosslinked with multifunctional crosslinking agents, Sep. Purif. Technol. 12 (1997) 145–156.
[88] V.S. Praptowidodo, Influence of swelling on water transport through PVA-based membrane, J. Mol. Struct. 739 (2005) 207–212.
[89] M.N. Hyder, R.Y.M. Huang, P. Chen, Correlation of physicochemical characteristics with pervaporation performance of poly(vinyl alcohol) membranes, J. Membr. Sci. 283 (2006) 281–290.
[90] H.A. Tsai, T.Y. Wang, S.H. Huang, C.C. Hu, W.S. Hung, K.R. Lee, J.Y. Lai, The preparation of polyamide/polyacrylonitrile thin film composite hollow fiber membranes for dehydration of ethanol mixtures, Sep. Purif. Technol. 187 (2017) 221–232.
[91] C. Cheng, P. Li, K. Shena, T. Zhang, X. Cao, B. Wang, X. Wang, B.S. Hsiao, Integrated polyamide thin-film nanofibrous composite membrane regulated by functionalized interlayer for efficient water/isopropanol separation, J. Membr. Sci. 553 (2018) 70–81.
[92] K. Mandal, S. Dutta, P.K. Bhattacharya, Characterization of blended polymeric membranes for pervaporation of hydrazine hydrate, Chem. Eng. J. 138 (2008) 10–19.
[93] A.K. Fard, G. McKay, A. Buekenhoudt, H. Al Sulaiti, F. Motmans, M. Khraisheh, M. Atieh, Inorganic Membranes: Preparation and Application for Water Treatment and Desalination, Materials 11 (2018) 11–57.
[94] Y. Morigami, M. Kondo, J. Abe, H. Kita, K. Okamoto, The first large-scale pervaporation plant using tubular-type module with zeolite NaA membrane, Sep. Purif. Technol. 25 (2001) 251–260.
[95] S. Sommer, T. Melin, Performance evaluation of microporous inorganic membranes in the dehydration of industrial solvents, Chem. Eng. Process. 44 (2005) 1138–1156.
[96] I.G. Wenten, P.T. Dharmawijaya, P.T.P. Aryanti, R.R. Mukti, Khoiruddin, LTA zeolite membranes: current progress and challenges in pervaporation, RSC Adv. 7 (2017) 29520–29539.
[97] H.L. Jamieson, H. Yin, A. Waller, A. Khosravi, M.L. Lind, Impact of acids on the structure and composition of Linde Type A zeolites for use in reverse osmosis membranes for recovery of urine-containing wastewaters, Micropor. Mesopor. Mat. 201 (2015) 50–60.
[98] F. Zhang, Y. Zheng, Hu. Lili, Hu. Na, M. Zhu, R. Zhou, X. Chen, H. Kita, Preparation of high-flux zeolite T membranes using reusable macroporous stainless steel supports in fluoride media, J. Membr. Sci 456 (2014) 107–116.
[99] H. Zhou, Y. Li, G. Zhu, J. Liu, W. Yang, Microwave-assisted hydrothermal synthesis of a&b-oriented zeolite T membranes and their pervaporation properties, Sep. Purif. Technol. 65 (2009) 164–172.
[100] Y. Luo, Y. Lv, P. Kumar, J. Chu, J. Yang, M. Tsapatsis, K.A. Mkhoyan, G. He, J. Lu, Y. Zhang, Epitaxial growth: rapid synthesis of highly permeable and selective zeolite-T membranes, J. Mater. Chem. A 5 (2017) 17828–17832.
[101] S.M. Mirfendereski, R. Daneshpour, T. Mohammadi, Synthesis and characterization of T-type zeolite membrane on a porous mullite tube, Desalination 200 (2006) 77–79.
[102] R.F. Zhou, L.L. Hu, Y.J. Zhang, N. Hu, X.S. Chen, X. Lin, H. Kita, Synthesis of oriented zeolite T membranes from clear solutions and their pervaporation properties, Micropor. Mesopor. Mat. 174 (2013) 81–89.
[103] K. Tanaka, R. Yoshikawa, C. Ying, H. Kita, K.I. Okamoto, Application of zeolite T membrane to vapor-permeation-aided esterification of lactic acid with ethanol, Chem. Eng. Sci. 57 (2002) 1577–1584.
[104] X. Wang, Y. Chen, C. Zhang, X. Gu, N. Xu, Preparation and characterization of high-flux T-type zeolite membranes supported on YSZ hollow fibers, J. Membr. Sci 455 (2014) 294–304.
[105] X. Wang, J. Jiang, D. Liu, Y. Xue, C. Zhang, X. Gu, Evaluation of hollow fiber T-type zeolite membrane modules for ethanol dehydration, Chin. J. Chem. Eng. 25 (2017) 581–586.
[106] M.M. Teoh, S. Bonyadi, T.S. Chung, Investigation of different hollow fiber module designs for flux enhancement in the membrane distillation process, J. Membr. Sci. 311 (2008) 371–379.
[107] D. Liu, G. Liu, L. Meng, Z. Dong, K. Huang, W. Jin, Hollow fiber modules with ceramic- supported PDMS composite membranes for pervaporation recovery of bio-butanol, Sep. Purif. Technol. 146 (2015) 24–32.
[108] K. Sato, K. Sugimoto, N. Shimotsuma, T. Kikuchi, T. Kyotani, T. Kurata, Development of practically available up-scaled high-silica CHA-type zeolite membranes for industrial purpose in dehydration of N-methyl pyrrolidone solution, J. Membr. Sci. 409–410 (2012) 82–95.
[109] C. Algieri, P. Bernardo, G. Golemme, G. Barbieri, E. Drioli, Permeation properties of a thin silicalite-1 (MFI) membrane, J. Membr. Sci. 222 (2003) 181–190.
[110] C. Algieri, G. Golemme, S. Kallus, J.D.F. Ramsay, Preparation of thin supported MFI membranes by in situ-nucleation and secondary growth, Micropor. Mesopor. Mater. 47 (2001) 127–134.
[111] H. Negishi, K. Sakaki, T. Ikegami, Silicalite pervaporation membrane exhibiting a separation factor of over 400 for butanol, Chem. Lett. 39 (2010) 1312–1314.
[112] Y. Li, G. Zhu, Y. Wang, Y. Chai, C. Liu, Preparation, mechanism and applications of oriented MFI zeolite membranes: A review, Microporous Mesoporous Mater. 312 (2021), 110790.
[113] S.M. Mirfendereski, J.Y.S. Lin, High-performance MFI zeolite hollow fiber membranes synthesized by double-layer seeding with variable temperature secondary growth, J. Membr. Sci. 618 (2021), 118573.
[114] H. Matsuda, H. Yanagishita, H. Negishi, D. Kitamoto, T. Ikegami, K. Haraya, T. Nakane, Y. Idemoto, N. Koura, T. Sano, Improvement of ethanol selectivity of silicalite membrane in pervaporation by silicone rubber coating, J. Membr. Sci. 210 (2002) 433–437.
[115] X. Lin, X. Chen, H. Kita, K. Okamoto, Synthesis of silicalite tubular membranes by in situ crystallization, AIChE J. 49 (2003) 237–247.
[116] M. Kanezashi, J. O'Brien, Y.S. Lin, Template-free synthesis of MFI-type zeolite membranes: Permeationcharacteristics and thermal stability improvement of membrane structure, J. Membr. Sci. 286 (2006) 213–222.
[117] J. Peng, Z. Zhan, L. Shan, X. Li, Z. Wang, Y. Yan, Preparation of zeolite MFI membranes on defective macroporous alumina supports by a novel wetting–rubbing seeding method: Role of wetting agent, J. Membr. Sci. 444 (2013) 60–69.
[118] S. Xia, Y. Peng, Z. Wang, Microstructure manipulation of MFI-type zeolite membranes on hollow fibers for ethanol–water separation, J. Membr. Sci. 498 (2016) 324–335.
[119] S. Li, V.A. Tuan, R.D. Noble, J.L. Falconer, Pervaporation of water/THF mixtures using zeolite membranes, Ind. Eng. Chem. Res. 40 (2001) 4577–4585.
[120] D. Shah, K. Kissick, A. Ghorpade, R. Hannah, D. Bhattacharyya, Pervaporation of alcohol-water and dimethylformamide-water mixtures using hydrophilic zeolite NaA membranes: mechanisms and experimental results, J. Membr. Sci. 179 (2000) 185–205.
[121] Y. Zhang, X. Zhu, S. Chen, J. Liu, Z. Hong, J. Wang, Z. Li, X. Gao, R. Xu, X. Gu, $TiO_2$-decorated NaA zeolite membranes with improved separation stability for pervaporation dehydration of N, N-Dimethylacetamide, J. Membr. Sci. 634 (2021), 119398.
[122] X. Zhang, X. Song, L. Qiu, M. Ding, N. Hu, R. Zhou, X. Chen, Synthesis and pervaporation performance of highly reproducible zeolite T membranes from clear solutions, Chi. J. Cat. 34 (2013) 542–547.
[123] D. Kunnakorna, T. Rirksomboona, P. Aungkavattan, N. Kuanchertchoo, D. Atong, K. Hemra, S. Kulprathipanja, S. Wongkasemjit, Optimization of synthesis time for high performance of NaA zeolite membranes synthesized via autoclave for water-ethanol separation, Desalination, Desalination 280 (2011) 259–265.
[124] J. Shao, Z. Zhan, J. Li, Z. Wang, K. Li, Y. Yan, Zeolite NaA membranes supported on alumina hollow fibers: Effect of support resistances on pervaporation performance, J. Membr. Sci. 451 (2014) 10–17.
[125] X. Gao, B. Gao, H. Liu, C. Zhang, Y. Zhang, J. Jiang, X. Gu, Fabrication of stainless steel hollow fiber supported NaA zeolite membrane by self-assembly of submicron seeds, Sep Pur. Tec. 234 (2020), 116121.
[126] Z. Xiaoliang, S. Xin, Q. Lingfang, D. Minzheng, H. Na, Z. Rongfei, C. Xiangshu, Synthesis and pervaporation performance of highly reproducible zeolite T membranes from clear solutions, Chi. J. Cat. 34 (2013) 542–547.
[127] Y. Hasegawa, C. Abe, M. Nishioka, K. Sato, T. Nagase, T. Hanaoka, Formation of high flux CHA-type zeolite membranes and their application to the dehydration of alcohol solutions, J. Membr. Sci. 264 (2010) 318–324.
[128] G. Zhu, Y. Li, H. Zhou, J. Liu, W. Yang, Microwave synthesis of high performance FAU-type zeolite membranes: Optimization, characterization and pervaporation dehydration of alcohols, J. Membr. Sci. 337 (2009) 47–54.
[129] H. Zhou, Y. Li, G. Zhu, J. Liu, W. Yang, Preparation of zeolite T membranes by microwave-assisted in situ nucleation and secondary growth, Mater. Lett. 63 (2009) 255–257.
[130] Y. Liu, X. Wang, Y. Zhang, Y. He, X. Gu, Scale-up of NaA zeolite membranes on$\alpha$-$Al_2O_3$ hollow fibers by a secondary growth method with vacuum seeding, Ch. J. Chem. Eng 23 (2015) 1114–1122.
[131] H. Zhou, D. Korelskiy, T. Leppäjärvi, M. Grahn, J. Tanskanen, J. Hedlund, Ultrathin zeolite X membranes for pervaporation dehydration of ethanol, J. Membr. Sci. 399 (2012) 106–111.
[132] A.A. Alomair, Y. Alqaheem, Optimization of mordenite membranes using sucrose precursor for pervaporation of water-ethanol mixtures, Membranes 11 (2021) 160.
[133] http://www.who.int/news-room/fact-sheets/detail/drinking-water.
[134] S.F. Anis, R. Hashaikeh, N. Hilal, Reverse osmosis pretreatment technologies and future trends: A comprehensive review, Desalination 452 (2019) 159–195.
[135] F. Macedonio, E. Drioli, Membrane engineering for green process engineering, Engineering 3 (2017) 290–298.

[136] B. Peñate, L. García-Rodríguez, Current trends and future prospects in the design of seawater reverse osmosis desalination technology, Desalination 284 (2012) 1–8.
[137] F. Macedonio, E. Drioli, Membrane systems for seawater and brackish water desalination, in: E. Drioli, L. Giorno, E. Fontananova (Eds.), Comprehensive Membrane Science and Engineering, second ed., Elsevier, Oxford, 2017, pp. 118–130.
[138] R.A. Clayton, Review of current knowledge, desalination for water supply, Foundation for Water Research, Marlow, UK, 2011.
[139] http://iea-etsap.org/E-TechDS/PDF/I12IR_Desalin_MI_Jan2013_final_GSOK.pdf.
[140] A. Matin, T. Laoui, W. Falath, M. Farooque, Fouling control in reverse osmosis for water desalination & reuse: Current practices & emerging environment-friendly technologies, Sci. Total. Environ. 765 (2021) 142721–142740.
[141] J.C.T. Lin, D.J. Lee, C. Huang, Membrane fouling mitigation: membrane cleaning, Sep. Sci. Technol. 45 (2010) 858–872.
[142] L.X. Li, J.H. Dong, T.M. Nenoff, R. Lee, Desalination by reverse osmosis using MFI zeolite membranes, J. Membr. Sci. 243 (2004) 401–404.
[143] L. Li, J. Dong, T.M. Nenoff, R. Lee, Reverse osmosis of ionic aqueous solutions on a MFI zeolite membrane, Desalination 170 (2004) 309–316.
[144] L. Li, N. Liu, B. McPherson, R. Lee, Enhanced water permeation of reverse osmosis through MFI-type zeolite membranes with high aluminum contents, Ind. Eng. Chem. Res. 46 (2007) 1584–1589.
[145] G. Golemme, A. Nastro, J.B. Nagy, B. Subotic, F. Crea, R. Aiello, Kinetic study on the nucleation of (Na, TPA)-ZSM-5 zeolite, Zeolites 11 (1991) 776–783.
[146] M. Duke, J. O'Brien-Abraham, N. Milne, B. Zhu, J.Y.S. Lin, J.C.D. da Costa, Seawater desalination performance of MFI type membranes made by secondary growth, Sep. Pur. Tech. 68 (2009) 343–350.
[147] C. Cho, K.Y. Oh, S.K. Kim, J.G. Yeo, P-. Sharma, Pervaporative seawater desalination using NaA zeolite membrane: mechanisms of high water flux and high salt rejection, J. Membr. Sci. 371 (2011) 226–238.
[148] M. Drobek, C. Yacou, J. Motuzas, A. Julbe, L. Ding, J.C.D. da Costa, Long term pervaporation desalination of tubular MFI zeolite membranes, J. Membr. Sci. 415–416 (2012) 816–823.
[149] B. Zhu, L. Zou, C.M. Doherty, A.J. Hill, Y.S. Lin, X. Hu, H. Wang, M. Duke, I Investigation of the effects of ion and water interaction on structure and chemistry of silicalite MFI type zeolite for its potential use as a seawater desalination membrane, J. Mater. Chem. 20 (2010) 4675–4683.
[150] B. Zhu, D.T. Myat, J.W. Shin, Y.H. Na, I.S. Moon, G. Connor, S. Maeda, G. Morris, S. Gray, Mikel Duke, Application of robust MFI-type zeolite membrane for desalination of saline wastewater, J. Membr. Sci. 475 (2015) 167–174.
[151] A. Alkhudhiri, N. Hilal, Air gap membrane distillation: A detailed study of high saline solution, Desalination 403 (2017) 179–186.
[152] M.H. Sharqawy, J.H. Lienhard, S.M. Zubair, Thermophysical properties of seawater: A review of existing correlations and data, Desalin. Water Treat. 16 (2012) 354–380.
[153] L. Donato, A. Garofalo, E. Drioli, O. Alharbi, S.A. Aljlil, A. Criscuoli, C. Algieri, Improved performance of vacuum membrane distillation in desalination with zeolite membranes, Sep. Purif. Technol. 237 (2020), 116376.
[154] X. Yan, C. Wang, Experimental study on vacuum membrane distillation based on brine desalination by PVDF, IOP Conference Series: Earth and Environmental Science 67 (2017), 012002.
[155] Y. Wang, H. Rong, L. Sun, P. Zhang, Y. Yang, L. Jiang, S. Wu, G. Zhu, X. Zou, Fabrication and evaluation of effective zeolite membranes for water desalination, Desalination 504 (2021), 114974.
[156] V. Martin-Gil, M.Z. Ahmad, R. Castro-Muñoz, V. Fila, Economic framework of membrane technologies for natural gas applications, Separ. Purif. Rev 48 (2019) 198–324.
[157] P. Bernardo, G. Clarizia, 30 Years of Membrane Technology for Gas Separation, Chem. Eng. Trans. 32 (2013) 1999–2004.
[158] Y. Liu, M. Li, Z. Chen, Y. Cui, J. Lu, Y. Liu, Hierarchy control of MFI zeolite membrane towards superior butane isomer separation performance, Angew. Chem. Int. Ed. 60 (2021) 7659–7663.
[159] B. Min, A. Korde, S. Yang, Y. Kim, C.W. Jones, S. Nair, Separation of $C_2$–$C_4$ hydrocarbons from methane by zeolite MFI hollow fiber membranes fabricated from 2D nanosheets, AIChE J. 67 (2021), e17048.
[160] L. Yu, S. Fouladvand, M. Grahn, J. Hedlund, Ultra-thin MFI membranes with different Si/Al ratios for CO2/CH4 separation, Micropor.b Mesopor. Mat.
[161] X. Gu, J. Dong, T.M. Nenoff, Synthesis of defect-free FAU-type zeolite membranes and separation for dry and moist CO2/N2 mixtures, Ind. Eng. Chem. Res. 44 (2005) 937–944.
[162] T. Wu, C. Shu, S. Liu, B. Xu, S. Zhong, Rongfei Zhou, Separation performance of Si-CHA zeolite membrane for a binary H2/CH4 mixture and ternary and quaternary mixtures containing impurities, Energ. Fuel. 34 (2020) 11650–11659.
[163] B. Liu, R. Zhang, Y. Du, F. Gao, J. Zhou, R. Zhou, Highly selective high-silica SSZ-13 zeolite membranes for H2 production from syngas, Int. J. Hydrog. Energy 45 (2020) 16210–16218.
[164] S.F. Alam, M.Z. Kim, Y.J. Kim, A. ur Rehman, A. Devipriyanka, P. Sharma, J. G. Yeo, J.S. Lee, H. Kim, C.H. Cho, A new seeding method, dry rolling applied to synthesize SAPO-34 zeolite membrane for nitrogen/methane separation, J. Membr. Sci. 602 (2020), 117825.
[165] https://www.snam.it/export/sites/snam-rp/repository/file/gas_naturale/global-gasreport/global_gas_report_2018.pdf.
[166] S. Faramawy, T. Zak, A.A.E. Sakr, Natural gas origin, composition, and processing: A review, J. Nat. Gas Sci. Eng. 34 (2016) 34–54.
[167] R.W. Baker, K. Lokhandwala, Natural gas processing with membranes: an overview, Ind. Eng. Chem. Res. 47 (2008) 2109–2121.
[168] C.A. Scholes, G.W. Stevens, S.E. Kentish, Membrane gas separation applications natural gas processing, Fuel 96 (2012) 15–28.
[169] D.M. D'Alessandro, B. Smit, J.R. Long, Carbon dioxide capture: prospects for new materials, Angew. Chem. Int. Ed. 49 (2010) 6058–6082.
[170] A.W. Ameen, P.M. Budd, P. Gorgojo, Superglassy polymers to treat natural gas by hybrid membrane/amine processes: Can fillers help? Membranes 10 (2020) 413–437.
[171] N. Norahim, P. Yaisanga, K. Faungnawakij, T. Charinpanit-kul, C. Klaysom, Recent membrane developments for $CO_2$ separation and capture, Chem. Eng. Technol. 41 (2018) 211–223.
[172] A. Iulianelli, E. Drioli, Membrane engineering: Latest advancements in gas separation and pre- T treatment processes, petrochemical industry and refinery, and future perspectives in emerging applications, Fuel Process. Technol. 206 (2020), 106464.
[173] M. Zhang, L. Deng, D. Xiang, B. Cao, S.S. Hossein, P, Li, Approaches to suppress $CO_2$-induced plasticization of polyimide membranes in gas separation applications, Processes 7 (2019) 51.
[174] W.J. Koros, R. Mahajan, Pushing the limits on possibilities for large-scale gas separation: which strategies? J. Membr. Sci. 175 (2000) 181–196.
[175] H. Kalipcilar, T.C. Bowen, R.D. Noble, J.L. Falconer, Synthesis and separation performance of SSZ-13 zeolite membranes on tubular supports, Chem. Mater. 14 (2002) 3458–3464.
[176] N. Kosinov, C. Auffret, C. Gücüyener, B.M. Szyja, J. Gascon, F. Kapteijn, E.J. M. Hensen, High flux high-silica SSZ-13 membrane for $CO_2$ separation, Mater. Chem. A 2 (2014) 13083–13092.
[177] K.C. Khulbe, T. Matsuura, C.Y. Feng, A.F. Ismail, Recent development on the effect of water/moisture on the performance of zeolite membrane and MMMs containing zeolite for gas separation; review, RSC Adv. 6 (2016) 42943–42961.
[178] K. Kida, Y. Maeta, K. Yogo, Pure silica CHA-type zeolite membranes for dry and humidified $CO_2/CH_4$ mixtures separation, Sep. Purif. Technol. 197 (2018) 116–121.
[179] N. Kosinov, C. Auffret, Gerard J. Borghuis, Venkata G.P. Sripathi, E.J.M. Hensen, Influence of the Si/Al ratio on the separation properties of SSZ-13 zeolite membranes, J. Membr. Sci. 484 (2015) 140–145.
[180] H. Imai, N. Hayashida, T. Yokoi, T. Tatsumi, Direct crystallization of CHA-type zeolite from amorphous aluminosilicate gel by seed-assisted method in the absence of organic-structure-directing agents, Micropor. Mesopor. Mat. 196 (2014) 341–348.
[181] S. Araki, Y. Okubo, K. Maekawa, S. Imasaka, H. Yamamoto, Preparation of a high-silica chabazite-type zeolite membrane with high $CO_2$ permeability using tetraethylammonium hydroxide, J. Membr. Sci. 613 (2020) 118480–118487.
[182] L. Yu, A. Holmgren, M. Zhou, J. Hedlund, Highly permeable CHA membranes prepared by fluoride synthesis for efficient $CO_2/CH_4$ separation, J. Mater. Chem. A 6 (2018) 6847–6853.
[183] M.J.D. Cabañas, P.A. Barrett, M.A. Camblor, Synthesis and structure of pure $SiO_2$ chabazite: the $SiO_2$ polymorph with the lowest framework density, Chem. Commun. 1881–1882 (1998).
[184] X. Zhu, N. Kosinov, J.P. Hofmann, B. Mezari, Q. Qian, R. Rohling, B. M. Weckhuysen, J. Ruiz-Martınez, E.J.M. Hensen, Fluoride-assisted synthesis of bimodal microporous SSZ-13 zeolite, Chem. Commun. 52 (2016) 3227–3230.
[185] Z. Lixiong, J. Mengdong, M. Enze, Synthesis of SAPO-34/ceramic composite membranes, Stud. Surf. Sci. Catal. 105 (1997) 2211–2216.
[186] S. Li, G. Alvarado, R.D. Noble, J.L. Falconer, Effects of impurities on $CO_2/CH_4$ separations through SAPO-34 membranes, J. Membr. Sci. 251 (2005) 59–66.
[187] M.A. Carreon, S. Li, J.L. Falconer, R.D. Noble, Alumina-supported SAPO-34 membranes for $CO_2/CH_4$, J. Am. Chem. Soc. 130 (2008) 5412–5413.
[188] S. Li, M.A. Carreon, Y. Zhang, H.H. Funke, R.D. Noble, J.L. Falconer, Scale-up of SAPO-34 membranes for $CO_2/CH_4$ separation, J. Membr. Sci. 352 (2010) 7–13.
[189] Y. Chen, Y. Zhang, C. Zhang, J. Jiang, X. Gu, Fabrication of high-flux SAPO-34 membrane on $\alpha$-$Al_2O_3$ four-channel hollow fibers for $CO_2$ capture from $CH_4$, J. $CO_2$ Util. 18 (2017) 30–40.
[190] R.U. Rehman, Q. Song, L. Peng, Y. Chen, X. Gu, Hydrophobic modification of SAPO-34 membranes for improvement of stability under wet condition Chin, J. Chem. Eng. 27 (2019) 2397–2406.
[191] R. Rehman, Q. Song, L. Peng, Z. Wu, X. Gu, A facile coating to intact SAPO-34 membranes for wet $CO_2/CH_4$ mixture separation, Chem. Eng. Res. Des. 153 (2020) 37–48.
[192] S. Qiu, M. Xue, G. Zhu, Metal-organic framework membranes: from synthesis to separation application, Chem. Soc. Rev. 43 (2014) 6116–6140.
[193] Z. Dai, L. Ansaloni, L. Deng, Recent advances in multi-layer composite polymeric membranes for $CO_2$ separation, Green Energy Environ. 1 (2016) 102–128.
[194] H. Gies, Studies on clathrasils IX: Crystal structure of decadodecasil 3 R, the missing link between zeolites and clathrasils, Z, Kristallogr. 175 (1986) 93–110.
[195] T. Tomita, K. Nakayama, H. Sakai, Gas separation characteristics of DDR type zeolite membrane, Micropor. Mesopor. Mat. 68 (2004) 71–75.
[196] S. Himeno, T. Tomita, K. Suzuki, K. Nakayama, K. Yajima, S. Yoshida, Synthesis and permeation properties of a DDR-type zeolite membrane for separation of $CO_2/CH_4$ gaseous mixtures, Ind. Eng. Chem. Res. 46 (2007) 6989–6997.
[197] S. Heng, P.P.S. Lau, K.L. Yeung, M. Djafer, J.C. Schrotter, Low-temperature ozone treatment for organic template removal from zeolite membrane, J. Membr. Sci. 243 (2004) 69–78.
[198] L. Wang, C. Zhang, X. Gao, L. Peng, J. Jiang, X. Gu, Preparation of defect-free DDR zeolite membranes by eliminating template with ozone at low temperature, J. Membr. Sci. 539 (2017) 152–160.
[199] N. Xu, D. Meng, X. Tang, X. Kong, L. Kong, Y. Zhang, H. Qiu, M. Wang, Y. Zhan, Fast synthesis of thin all-silica DDR zeolite membranes with inorganic base as

mineralizing agent for $CO_2$-$CH_4$ separation, Sep. Purif. Technol. 253 (2020), 117505.
[200] A. Brunetti, H. Maghsoudi, G. Barbieri, $CO_2$ separation from binary mixtures of $CH_4$, $N_2$, and $H_2$ by using SSZ-13 zeolite membrane, Sep. Purif. Technol. 256 (2021), 117796.
[201] H. Qiu, Y. Zhang, L. Kong, X. Kong, X. Tang, D. Meng, N. Xu, M. Wang, Y. Zhang, High performance SSZ-13 membranes prepared at low temperature, J. Membr. Sci. 603 (2020), 118023.
[202] B. Wang, Y. Zheng, J. Zhang, W. Zhang, F. Zhang, W. Xing, R. Zhou, High performance SSZ-13 membranes prepared at low temperature, Micropor. Mesopor. Mat. 275 (2019) 191–199.
[203] J. Zhou, F. Gao, K. Sun, X. Jin, Y. Zhang, B. Liu, R. Zhou, Green synthesis of highly $CO_2$–selective CHA zeolite membranes in all-silica and fluoride-free solution for $CO_2$/$CH_4$ separations, Energy & Fuels 34 (2020) 11307–11314.
[204] Y. Zhang, M. Wang, H. Qiu, L. Kong, N. Xu, X. Tang, D. Meng, X. Kong, Y. Zhang, Synthesis of thin SAPO-34 zeolite membranes in concentrated gel, J. Membr. Sci. 603 (2020), 118451.
[205] Y. Mu, H. Chen, H. Xiang, L. Lan, Y. Shao, X. Fan, C. Hardacre, Defects-healing of SAPO-34 membrane by post-synthesis modification using organosilica for selective $CO_2$ separation, J. Membr. Sci. 579 (2019) 80–88.
[206] N.M. Nguyen, Q.T. Le, D.P.H. Nguyen, T.N. Nguyen, T.T. Le, T.C.T. Pham, Facile synthesis of seed crystals and gelless growth of pure silica DDR zeolite membrane on low cost silica support for high performance in $CO_2$ separation, J. Membr. Sci. 624 (2021), 119110.
[207] M. Wang, L. Bai, M. Li, L. Gao, M. Wang, P. Rao, Y. Zhang, Ultrafast synthesis of thin all-silica DDR zeolite membranes by microwave heating, J. Membr. Sci. 15 (2019) 567–579.
[208] C. Algieri, G. Coppola, D. Mukherjee, M.I. Shammas, V. Calabrò, S. Curcio, S. Chakraborty, Catalytic membrane reactors: The industrial applications perspective, Catalysts 11 (2021) 691.
[209] A. Helmi, F. Gallucci, Latest developments in membrane (bio)reactors, Processes 8 (2020) 1239.
[210] T. Westermann, T. Melin, Flow through catalytic membrane reactors: principles and applications, Chem. Eng. Process 48 (2009) 17–28.
[211] A. Julbe, D. Farrusseng, C. Guizard, Porous ceramic membranes for catalytic reactor -overview and new ideas, J. Membr. Sci. 181 (2001) 3–20.
[212] G. Leonzio, Methanol synthesis: optimal solution for a better efficiency of the process, Processes 6 (2018) 20.
[213] B.F.K. Kingsbury, Z. Wu, K. Li, A Morphological Study of Ceramic Hollow Fiber Membranes: a Perspective on Multifunctional Catalytic Membrane Reactors, Catal. Today 156 (2010) 306–315.
[214] J. Caro, K.J. Caspary, C. Hamel, B. Hoting, P. Kolsch, B. Langanke, K. Nassauer, K. T. Schiestel, O.A. Schmidt, R. Schomacker, A. Seidel-Morgenstern, E. Tsotsas, I. Voigt, H. Wang, R. Warsitz, W. Steffen, A. Wolf, Catalytic membrane reactors for partial oxidation using perovskite hollow fiber membranes and for partial hydrogenation using a catalytic membrane contactor, Ind. Eng. Chem. Res. 46 (2007) 2286–2294.
[215] L. Chen, Z. Qi, S. Zhang, J. Su, G.A. Somorjai, Catalytic hydrogen production from methane: A review on recent progress and prospect, Catalysts 10 (2020) 858.
[216] G. Franchi, M. Capocelli, M. De Falco, V. Piemonte, D. Barba, Hydrogen production via steam reforming: A critical analysis of MR and RMM Technologies, Membranes 10 (2020) 10.
[217] J. Catalano, F. Guazzone, I.P. Mardilovich, N.K. Kazantzis, Y.H. Ma, Hydrogen production in a large scale water-gas shift Pd-based catalytic membrane reactor, Ind. Eng. Chem. Res. 52 (2013) 1042–1055.
[218] A.S. Augustine, Y.H. Ma, N.K. Kazantzis, High pressure palladium membrane reactor for the high temperature water gas shift reaction, Int. J. Hydrog. Energy 36 (2011) 5350–5360.
[219] S.J. Kim, S. Yang, G.K. Reddy, P. Smirniotis, J. Dong, Zeolite membrane reactor for high-temperature water-gas shift reaction: effects of membrane properties and operating conditions, Energy Fuels 27 (2013) 4471–4480.
[220] X. Gu, Z. Tang, J. Dong, On-stream modification of MFI zeolite membranes for enhancing hydrogen separation at high temperature, Micropor. Mesopor. Mat. 111 (2008) 441–448.
[221] A. Arvanitis, X. Sun, S. Yang, D. Damma, P. Smirniotis, J. Dong, Approaching complete CO conversion and total $H_2$ recovery for water gas shift reaction in a high-temperature and high-pressure zeolite membrane reactor, J. Membr. Sci. 549 (2018) 575–580.
[222] X. Gu, J. Dong, Tina M. Nenoff, D.E. Ozokwelu, Separation of p-Xylene from multicomponent vapor mixtures using tubular MFI zeolite membranes, Stud. Surf. Sci, Catal. 170 (2007) 949–954.
[223] Y. Zhang, Q. Sun, X. Gu, Pure H2 production through hollow fiber hydrogen-selective MFI zeolite membranes using steam as sweep Gas, AlChE J. 61 (2015) 3459–3460.
[224] Y. Zhang, Z. Wu, Z. Hong, X. Gu, N. Xu, Hydrogen-selective zeolite membrane reactor for low temperature water gas shift reaction, Chem. Eng. J. 197 (2012) 314–321.
[225] Z. Tang, S.J. Kim, G.K. Reddy, J. Dong, P. Smirniotis, Modified zeolite membrane reactor for high temperature water gas shift reaction, J. Membr. Sci. 354 (2010) 114–122.
[226] S.J. Kim, Z. Xu, G.K. Reddy, P. Smirniotis, J. Dong, Effect of pressure on high-temperature water gas shift reaction in microporous zeolite membrane reactor, Ind. Eng. Chem. Res. 51 (2012) 1364–1375.
[227] A. Rafiee, K.R. Khalilpour, D. Milani, M. Panahi, Trends in $CO_2$ conversion and utilization: A review from process systems perspective, J. Environ Chem. Eng. 6 (2018) 5771–5794.
[228] P. Rodriguez-Vega, A. Ateka, I. Kumakiri, H. Vicente, J. Ereña, A.T. Aguayo, J. Bilbao, Experimental implementation of a catalytic membrane reactor for the direct synthesis of DME from $H_2$+$CO/CO_2$, Chem. Eng. Sci. 234 (2021), 116396.
[229] I. Iliuta, F. Larachi, P. Fongarland, Dimethyl ether synthesis with in situ H2O removal in fixed-bed membrane reactor: Model and simulations, Ind. Eng. Chem. Res. 49 (2010) 6870–6877.
[230] D.A. Fedosov, A.V. Smirnov, V.V. Shkirskiy, T. Voskoboynikov, I.I. Ivanova, Methanol dehydration in NaA zeolite membrane reactor, J. Membr. Sci. 486 (2015) 189–194.
[231] Chen Zhou, Nanyi Wang, Yanan Qian, Xiaoxing Liu, Jurgen Caro, Aisheng Huang, Efficient synthesis of dimethyl ether from methanol in a bifunctional zeolite membrane reactor, Angew. Chem. 55 (2016) 12678–12682.
[232] H. Mahmoudi, M. Mahmoudi, O. Doustdar, H. Jahangiri, A. Tsolakis, S. Gu, M. L. Wyszynski, A review of Fischer Tropsch synthesis process, mechanism, surface chemistry and catalyst formulation, Biofuels Eng. 2 (2017) 11–31.
[233] M.P. Rohde, D. Unruh, G. Schaub, Membrane application in Fischer-Tropsch synthesis extractors-overview of concepts, Catal. Today 106 (2005) 143–148.
[234] S. Liu, B. Zhang, G. Liu, Metal-based catalysts for the non-oxidative dehydrogenation of light alkanes to light olefins, React. Chem. Eng. 6 (2021) 9–26.
[235] E. Mc Farland, Unconventional chemistry for unconventional natural gas, Science 338 (2012) 340–342.
[236] I. Amghizar, L.A. Vandewalle, K.M. Van Geem, G.B. Marin, New trends in olefin production, Engineering 3 (2017) 171–178.
[237] A. Farshi, F. Shaiyegh, S.H. Burogerdi, A. Dehgan, FCC process role in propylene demands, Pet. Sci. Technol. 29 (2011) 875–885.
[238] S.J. Kim, Y. Liu, J.S. Moore, R.S. Dixit, J.G. Pendergas Jr., D. Sholl, C.W. Jones, S. Nair, Thin hydrogen-selective SAPO-34 zeolite membranes for enhanced conversion and selectivity in propane dehydrogenation membrane reactors, Chem. Mater. 28 (2016) 4397–4402.
[239] D. Alihellal, L. Chibane, Comparative study of the performance of Fischer-Tropsch synthesis in conventional Packed Bed and in membrane reactor over iron- and cobalt-based catalysts, Arab. J. Sci Eng. 41 (2016) 357–369.
[240] S. Dangwal, R. Liu, S.J. Kim, High-temperature ethane dehydrogenation in microporous zeolite membrane reactor: Effect of operating conditions, Chem. Eng. J. 328 (2017) 862–872.
[241] S. Dangwal, R. Liu, S. Gaikwad, S.L. Han, S.J. Kim, Zeolite membrane reactor for high-temperature isobutane dehydrogenation reaction: Experimental and modeling studies, Chem. Eng. Process 142 (2019), 107583.
[242] S. Dangwal, R. Liu, S.V. Kirk, S.J. Kim, Effect of pressure on ethane dehydrogenation in MFI zeolite membrane reactor, Energy Fuels 32 (2018) 4628–4637.
[243] S. Mota, S. Miachon, J.C. Volta, J.A. Dalmon, Membrane reactor for selective oxidation of butane to maleic anhydride, Catal. Today 67 (2001) 169–176.
[244] A. Cruz-Lopez, N. Guilhaume, S. Miachon, J.A. Dalmon, Selective oxidation of butane to maleic anhydride in a catalytic membrane reactor adapted to rich butane feed, Catal. Today 107–108 (2005) 949–956.
[245] P. Bernardo, C. Algieri, E. Drioli, G. Barbieri, Catalytic (Pt-Y) membranes for the purification of $H_2$-rich stream, Catal. Today 118 (2006) 90–97.
[246] P. Bernardo, C. Algieri, G. Barbieri, E. Drioli, Hydrogen purification from carbon monoxide by means of selective oxidation using zeolite catalytic membranes, Sep. Purif. Technol. 62 (2008) 629–635.
[247] A. Manasilp, E. Gulari, Selective CO oxidation over Pt/alumina catalysts for fuel cell applications, Appl. Catal. B Environ. 37 (2002) 17–25.
[248] J.A. Medrano, A. Garofalo, L. Donato, F. Basile, M.P. De Santo, F. Gallucci, F. Cofone, F. Ciuchi, C. Algieri, CO selective oxidation using catalytic zeolite membranes, Chem. Eng. J. 351 (2018) 40–47.
[249] S. Masudy-Panah, R. Katal, N.D. Khiavi, E. Shekarian, J. Hu, X. Gong, J. Mater. Chem. A 39 (2019) 22332.
[250] X.B. Cheng, R. Zhang, C.Z. Zhao, Q. Zhang, Toward safe lithium metal anode in rechargeable batteries: a review, Chem. Rev. 117 (2017) 10403–10473.
[251] Y. Li, X. Wang, S. Dong, X. Chen, G. Cui, Recent advances in non-aqueous electrolyte for rechargeable Li–$O_2$ batteries, Adv. Energy Mater. 6 (2016) 1600751.
[252] A. Manthiram, X. Yu, S. Wang, Lithium battery chemistries enabled by solid-state electrolytes, Nat. Rev. Mater. 2 (2017) 16103.
[253] F. Han, A.S. Westover, J. Yue, X. Fan, F. Wang, M. Chi, D.N. Leonard, N. J. Dudney, H. Wang, C. Wang, Nat. Energy 4 (2019) 187–196.
[254] H. Liu, X.B. Cheng, J.Q. Huang, H. Yuan, Y. Lu, C. Yan, G.L. Zhu, R. Xu, C.Z. Zhao, L.P. Hou, C. He, S. Kaskel, Q. Zhang, Controlling dendrite growth in solid-state electrolytes, ACS Energy Lett. 5 (2020) 833–843.
[255] T. Famprikis, P. Canepa, J.A. Dawson, M.S. Islam, C. Masquelier, Fundamentals of inorganic solid-state electrolytes for batteries, Nat. Mater. 18 (2019) 1278–1291.
[256] S. Xia, X. Wu, Z. Zhang, Y. Cui, W. Liu, Practical challenges and future perspectives of all-solid-state lithium-metal batteries, Chem. 5 (2019) 753–785.
[257] X. Chi, M. Li, J. Di, P. Bai, L. Song, X. Wang, F. Li, S. Liang, J. Xu, J. Yu, A highly stable and flexible zeolite electrolyte solid-state Li–air battery, Nature 592 (2021) 551–557.
[258] Z. Wang, Q. Ge, J. Shao, Y. Yan, Y High performance zeolite LTA pervaporation membranes on ceramic hollow fibers by dip-coating-wiping seed deposition, J. Am. Chem. Soc. 131 (2009) 6910–6911.
[259] K. Ueno, J.W. Park, A. Yamazaki, T. Mandai, N. Tachikawa, K. Dokko, M. Watanabe, Anionic effects on solvate ionic liquid electrolytes in rechargeable lithium–sulfur batteries, J. Phys. Chem. C. 117 (2013) 20509–20516.
[260] J.W. Park, S.C. Jo, M.J. Kim, I.H. Choi, B.G. Kim, Y.J. Lee, H.Y. Choi, S. Kang, T. Y. Kim, K.J. Baeg, Flexible high-energy-density lithium-sulfur batteries using

nanocarbon-embedded fibrous sulfur cathodes and membrane separators, NPG Asia Mat. 13 (2021) 13.
[261] Y. Diao, K. Xie, S. Xiong, X. Hong, Insights into Li-S battery cathode capacity fading mechanisms: irreversible oxidation of active mass during cycling, J. Electrochem. Soc. 159 (2012) A1816–A1821.
[262] J. Han, H. Jang, H.T. Bui, M. Jahn, D. Ahn, K. Cho, B. Jun, S.U. Lee, S. Sabine, M. Stöger-Pollach, K. Whitmore, M.M. Sung, V. Kutwade, R. Sharma, S.H. Han, Stable performance of Li-S battery: Engineering of $Li_2S$ smart cathode by reduction of multilayer graphene-embedded 2D-$MoS_2$, J. Alloys Compd. 862 (5) (2021), 158031.
[263] W. Kang, N. Deng, J. Ju, Q. Li, D. Wu, X. Ma, L. Li, M. Naebe, B. Cheng, A review of recent developments in rechargeable lithium-sulfur batteries, Nanoscale 8 (2016) 16541–16588.
[264] M.Y. Wang, S.H. Han, Z.S. Chao, S.Y. Li, B. Tan, J.X. Lai, Z.Y. Guo, X.L. Wei, H. G. Jin, W.B. Luo, W.J. Yi, J.C. Fan, Celgard-supported LiX zeolite membrane as ion-permselective separator in lithium sulfur battery, J. Membr. Sci. 611 (2020), 118386.
[265] https://nspires.nasaprs.com/external/ (accessed on June 14, 2021).
[266] http://www.esa.int/Science_Exploration/Human_and_Robotic_Exploration/Exploration/ExoMars/What_is_ExoMars (accessed on June 14, 2021).
[267] https://spacenews.com/china-russia-enter-mou-on-international-lunar-research-station/ (accessed on June 14, 2021).
[268] G.S. Martin, G.K. Muellner, Report on aircraft oxygen generation, SAB-TR-11-04, USAF Scientific Advisory Board (2012) 1–238.
[269] https://www.nasa.gov/pdf/146558main_RecyclingEDA(final)%204_10_06.pdf (accessed on June 12, 2021).
[270] M.L. Perry, T.F. Fuller, A historical perspective of fuel cell technology in the 20th century, J. Electrochem. Soc. 149 (2002) S59–S67.
[271] https://www.nasa.gov/centers/glenn/technology/fuel_cells.html.
[272] B. North, O. Stoll, Space Shuttle Environmental Control and Life Support Systems, in: the Proceedings of the 7 Annual Meeting and Technical Display, American Institute of Aeronautics and Astronautics, Huston, Texas, US, 1970.
[273] Z. Zhan, C. Wang, W. Fu, M. Pan, Visualization of water transport in a transparent PEMFC, Int. J. Hydrog. Energy 37 (2012) 1094–1105.
[274] https://ui.adsabs.harvard.edu/abs/2003JPS...118...44M/abstract (accessed on June 15, 2021).
[275] A. Tang, L. Crisci, J. Jankovic, An overview of bipolar plates in proton exchange membrane fuel cells, Renew. Sust. Energ. Rev. 13 (2021), 022701.
[276] P. Bernardo, A. Iulianelli, F. Macedonio, E. Drioli, Membrane technologies for Space engineering, J. Membr. Sci. 626 (2021), 119177.
[277] B. Yang, W. Yuan, X. He, K. Ren, Air dehumidification by hollow fibre membrane with chilled water for spacecraft applications, Indoor Built Environ. 25 (2016) 758–771.
[278] M.R.H. Abdel-Salam, R.W. Besant, C.J. Simonson, Sensitivity of the performance of a flat-plate liquid-to-air membrane energy exchanger (LAMEE) to the air and solution channel widths and flow maldistribution, Int. J. Heat Mass Transf. 84 (2015) 10821100.
[279] F.L. Liu, J.C. Su, X. Cui, S.C. Zhang, X.Z. Meng, L.W. Jin, Nanoparticles filled PVA/PVDF hollow fiber membrane towards enhanced performance for air dehumidification, IOP Conf. Series: Earth and Environmental, Science 463 (2020), 012096.
[280] W. Liu, Molecular sieve membranes made in thin sheet form, TechConnect Briefs 2018 -, Advanced Materials (2018) 232–235.
[281] R. Xing, Y. Rao, W.T. Grotenhuis, N. Canfield, F. Zheng, D.W. Winiarski, W. Liu, Advanced thin zeolite/metal flat sheet membrane for energy efficient air dehumidification and conditioning, Chem. Eng. Sci. 104 (2013) 595–609.
[282] https://techport.nasa.gov/view/16846 (accessed on June 10, 2021).
[283] A. Zachopoulos, E. Heracleous, Overcoming the equilibrium barriers of CO hydrogenation to methanol via water sorption: A thermodynamic analysis, J. CO2 Util. 21 (2017) 360–367.
[284] M. Bayat, Z. Dehghani, M.R. Rahimpour, Membrane/sorption-enhanced methanol synthesis process: Dynamic simulation and optimization, J. Ind. Eng. Chem. 20 (5) (2014) 3256–3269.
[285] A.C. Faria, C.V. Miguel, L.M. Madeira, Thermodynamic analysis of the CO methanation reaction with in situ water removal for biogas upgrading, Journal of $CO_2$ Utilization 26 (2018) 271–280.
[286] A.C. Faria, C.V. Miguel, A.E. Rodrigues, L.M. Madeira, Modeling and simulation of a steam-selective membrane reactor for enhanced $CO_2$ methanation, Ind. Eng. Chem. Res. 59 (2020) 16170–16184.
[287] T. Ghidini, Materials for Space exploration and settlement, Nature Mat. 17 (2018) 846–850.
[288] https://ntrs.nasa.gov/citations/20190025149 (Accessed on June 15, 2021).
[289] A. Miteva, V. Stoyanova, Zeolites application in terrestrial and space industry-a review, Aerosp. Res. Bulgaria 32 (2020) 209–233.